to Luigi Naldini (San Raffaele Telethon Institute for Gene Therapy) and Kenzaburo Tani (Kyushu University) for providing the VSV-G envelope-expressing plasmid (pMD-G).

This work was supported by Grants-in-Aid from the Japan Human Sciences Foundation.

REFERENCES

1. **Adachi, A., H. E. Gendelman, S. Koenig, T. Folks, R. Willey, A. Rabson, and M. A. Martin.** 1986. Production of acquired immunodeficiency syndrome-associated retrovirus in human and nonhuman cells transfected with an infectious molecular clone. J. Virol. **59**:284–291.
2. **Aiken, C.** 1997. Pseudotyping human immunodeficiency virus type 1 (HIV-1) by the glycoprotein of vesicular stomatitis virus targets HIV-1 entry to an endocytic pathway and suppresses both the requirement for Nef and the sensitivity to cyclosporin A. J. Virol. **71**:5871–5877.
3. **Alonso, A., T. P. Cujec, and B. M. Peterlin.** 1994. Effects of human chromosome 12 on interactions between Tat and TAR of human immunodeficiency virus type 1. J. Virol. **68**:6505–6513.
4. **Alonso, A., D. Derse, and B. M. Peterlin.** 1992. Human chromosome 12 is required for optimal interactions between Tat and TAR of human immunodeficiency virus type 1 in rodent cells. J. Virol. **66**:4617–4621.
5. **Bai, Y., Y. Soda, K. Izawa, T. Tanabe, X. Kang, A. Tojo, H. Hoshino, H. Miyoshi, S. Asano, and K. Tani.** 2003. Effective transduction and stable transgene expression in human blood cells by a third-generation lentiviral vector. Gene Ther. **10**:1446–1457.
6. **Balliet, J. W., D. L. Kolson, G. Eiger, F. M. Kim, K. A. McGann, A. Srinivasan, and R. Collman.** 1994. Distinct effects in primary macrophages and lymphocytes of the human immunodeficiency virus type 1 accessory genes vpr, vpu, and nef: mutational analysis of a primary HIV-1 isolate. Virology **200**:623–631.
7. **Baumann, J. G., D. Unutmaz, M. D. Miller, S. K. Breun, S. M. Grill, J. Mirro, D. R. Littman, A. Rein, and V. N. KewalRamani.** 2004. Murine T cells potently restrict human immunodeficiency virus infection. J. Virol. **78**:12537–12547.
8. **Benit, L., N. De Parseval, J. F. Casella, I. Callebaut, A. Cordonnier, and T. Heidmann.** 1997. Cloning of a new murine endogenous retrovirus, MuERV-L, with strong similarity to the human HERV-L element and with a gag coding sequence closely related to the Fv1 restriction gene. J. Virol. **71**:5652–5657.
9. **Berson, J. F., D. Long, B. J. Doranz, J. Rucker, F. R. Jirik, and R. W. Doms.** 1996. A seven-transmembrane domain receptor involved in fusion and entry of T-cell-tropic human immunodeficiency virus type 1 strains. J. Virol. **70**:6288–6295.
10. **Best, S., P. Le Tissier, G. Towers, and J. P. Stoye.** 1996. Positional cloning of the mouse retrovirus restriction gene Fv1. Nature **382**:826–829.
11. **Bieniasz, P. D., and B. R. Cullen.** 2000. Multiple blocks to human immunodeficiency virus type 1 replication in rodent cells. J. Virol. **74**:9868–9877.
12. **Bouyac-Bertoia, M., J. D. Dvorin, R. A. Fouchier, Y. Jenkins, B. E. Meyer, L. I. Wu, M. Emerman, and M. H. Malim.** 2001. HIV-1 infection requires a functional integrase NLS. Mol. Cell **7**:1025–1035.
13. **Browning, J., J. W. Horner, M. Pettoello-Mantovani, C. Raker, S. Yurasov, R. A. DePinho, and H. Goldstein.** 1997. Mice transgenic for human CD4 and CCR5 are susceptible to HIV infection. Proc. Natl. Acad. Sci. USA **94**:14637–14641.
14. **Bukrinsky, M., K. Manogue, and A. Cerami.** 1995. HIV results in the frame. Other approaches. Nature **375**:195–196. (Author's reply, **375**:198.)
15. **Cherepanov, P., G. Maertens, P. Proost, B. Devreese, J. Van Beeumen, Y. Engelborghs, E. De Clercq, and Z. Debyser.** 2003. HIV-1 integrase forms stable tetramers and associates with LEDGF/p75 protein in human cells. J. Biol. Chem. **278**:372–381.
16. **Connor, R. I., B. K. Chen, S. Choe, and N. R. Landau.** 1995. Vpr is required for efficient replication of human immunodeficiency virus type-1 in mononuclear phagocytes. Virology **206**:935–944.
17. **Cullen, B. R.** 2001. Journey to the center of the cell. Cell **105**:697–700.
18. **Depienne, C., A. Mousnier, H. Leh, E. Le Rouzic, D. Dormont, S. Benichou, and C. Dargemont.** 2001. Characterization of the nuclear import pathway for HIV-1 integrase. J. Biol. Chem. **276**:18102–18107.
19. **Depienne, C., P. Roques, C. Creminon, L. Fritsch, R. Casseron, D. Dormont, C. Dargemont, and S. Benichou.** 2000. Cellular distribution and karyophilic properties of matrix, integrase, and Vpr proteins from the human and simian immunodeficiency viruses. Exp. Cell Res. **260**:387–395.
20. **Farnet, C. M., B. Wang, J. R. Lipford, and F. D. Bushman.** 1996. Differential inhibition of HIV-1 preintegration complexes and purified integrase protein by small molecules. Proc. Natl. Acad. Sci. USA **93**:9742–9747.
21. **Fassati, A., D. Gorlich, I. Harrison, L. Zaytseva, and J. M. Mingot.** 2003. Nuclear import of HIV-1 intracellular reverse transcription complexes is mediated by importin 7. EMBO J. **22**:3675–3685.
22. **Feng, Y., C. C. Broder, P. E. Kennedy, and E. A. Berger.** 1996. HIV-1 entry cofactor: functional cDNA cloning of a seven-transmembrane, G protein-coupled receptor. Science **272**:872–877.
23. **Fouchier, R. A., B. E. Meyer, J. H. Simon, U. Fischer, and M. H. Malim.** 1997. HIV-1 infection of non-dividing cells: evidence that the amino-terminal basic region of the viral matrix protein is important for Gag processing but not for post-entry nuclear import. EMBO J. **16**:4531–4539.
24. **Gabuzda, D. H., H. Li, K. Lawrence, B. S. Vasir, K. Crawford, and E. Langhoff.** 1994. Essential role of vif in establishing productive HIV-1 infection in peripheral blood T lymphocytes and monocyte/macrophages. J. Acquir. Immune Defic. Syndr. **7**:908–915.
25. **Gallay, P., T. Hope, D. Chin, and D. Trono.** 1997. HIV-1 infection of nondividing cells through the recognition of integrase by the importin/karyopherin pathway. Proc. Natl. Acad. Sci. USA **94**:9825–9830.
26. **Garber, M. E., and K. A. Jones.** 1999. HIV-1 Tat: coping with negative elongation factors. Curr. Opin. Immunol. **11**:460–465.
27. **Garber, M. E., P. Wei, V. N. KewalRamani, T. P. Mayall, C. H. Herrmann, A. P. Rice, D. R. Littman, and K. A. Jones.** 1998. The interaction between HIV-1 Tat and human cyclin T1 requires zinc and a critical cysteine residue that is not conserved in the murine CycT1 protein. Genes Dev. **12**:3512–3527.
28. **Goff, S. P.** 1996. Operating under a Gag order: a block against incoming virus by the Fv1 gene. Cell **86**:691–693.
29. **Habu, K., J. Nakayama-Yamada, M. Asano, S. Saijo, K. Itagaki, R. Horai, H. Yamamoto, T. Sekiguchi, T. Nosaka, M. Hatanaka, and Y. Iwakura.** 1999. The human T cell leukemia virus type I-tax gene is responsible for the development of both inflammatory polyarthropathy resembling rheumatoid arthritis and noninflammatory ankylotic arthropathy in transgenic mice. J. Immunol. **162**:2956–2963.
30. **Hart, C. E., C. Y. Ou, J. C. Galphin, J. Moore, L. T. Bacheler, J. J. Wasmuth, S. R. Petteway, Jr., and G. Schochetman.** 1989. Human chromosome 12 is required for elevated HIV-1 expression in human-hamster hybrid cells. Science **246**:488–491.
31. **Hatziioannou, T., S. Cowan, and P. D. Bieniasz.** 2004. Capsid-dependent and -independent postentry restriction of primate lentivirus tropism in rodent cells. J. Virol. **78**:1006–1011.
32. **Heinzinger, N. K., M. I. Bukinsky, S. A. Haggerty, A. M. Ragland, V. Kewalramani, M. A. Lee, H. E. Gendelman, L. Ratner, M. Stevenson, and M. Emerman.** 1994. The Vpr protein of human immunodeficiency virus type 1 influences nuclear localization of viral nucleic acids in nondividing host cells. Proc. Natl. Acad. Sci. USA **91**:7311–7315.
33. **Ho, S. N., H. D. Hunt, R. M. Horton, J. K. Pullen, and L. R. Pease.** 1989. Site-directed mutagenesis by overlap extension using the polymerase chain reaction. Gene **77**:51–59.
34. **Hogan, B., E. Constantini, and E. Lacey.** 1994. Manipulating the mouse embryo: a laboratory manual, 2nd ed. Cold Spring Harbor Laboratory Press, Cold Spring Harbor, NY.
35. **Isegawa, Y., J. Sheng, Y. Sokawa, K. Yamanishi, O. Nakagomi, and S. Ueda.** 1992. Selective amplification of cDNA sequence from total RNA by cassette-ligation mediated polymerase chain reaction (PCR): application to sequencing 6.5 kb genome segment of hantavirus strain B-1. Mol. Cell Probes **6**:467–475.
36. **Iwakura, Y., T. Shioda, M. Tosu, E. Yoshida, M. Hayashi, T. Nagata, and H. Shibuta.** 1992. The induction of cataracts by HIV-1 in transgenic mice. AIDS **6**:1069–1075.
37. **Jackson, J. B., K. L. MacDonald, J. Cadwell, C. Sullivan, W. E. Kline, M. Hanson, K. J. Sannerud, S. L. Stramer, N. J. Fildes, S. Y. Kwok, et al.** 1990. Absence of HIV infection in blood donors with indeterminate western blot tests for antibody to HIV-1. N. Engl. J. Med. **322**:217–222.
38. **Jolicoeur, P., and D. Baltimore.** 1976. Effect of Fv-1 gene product on proviral DNA formation and integration in cells infected with murine leukemia viruses. Proc. Natl. Acad. Sci. USA **73**:2236–2240.
39. **Jolicoeur, P., and E. Rassart.** 1980. Effect of Fv-1 gene product on synthesis of linear and supercoiled viral DNA in cells infected with murine leukemia virus. J. Virol. **33**:183–195.
40. **Keppler, O. T., W. Yonemoto, F. J. Welte, K. S. Patton, D. Iacovides, R. E. Atchison, T. Ngo, D. L. Hirschberg, R. F. Speck, and M. A. Goldsmith.** 2001. Susceptibility of rat-derived cells to replication by human immunodeficiency virus type 1. J. Virol. **75**:8063–8073.
41. **Klatzmann, D., E. Champagne, S. Chamaret, J. Gruest, D. Guetard, T. Hercend, J. C. Gluckman, and L. Montagnier.** 1984. T-lymphocyte T4 molecule behaves as the receptor for human retrovirus LAV. Nature **312**:767–768.
42. **Koito, A., Y. Kameyama, C. Cheng-Mayer, and S. Matsushita.** 2003. Susceptibility of mink (Mustera vision)-derived cells to replication by human immunodeficiency virus type 1. J. Virol. **77**:5109–5117.
43. **Koito, A., H. Shigekane, and S. Matsushita.** 2003. Ability of small animal cells to support the postintegration phase of human immunodeficiency virus type-1 replication. Virology **305**:181–191.
44. **Kukolj, G., K. S. Jones, and A. M. Skalka.** 1997. Subcellular localization of avian sarcoma virus and human immunodeficiency virus type 1 integrases. J. Virol. **71**:843–847.
45. **Kwok, S., D. E. Kellogg, N. McKinney, D. Spasic, L. Goda, C. Levenson, and J. J. Sninsky.** 1990. Effects of primer-template mismatches on the polymerase chain reaction: human immunodeficiency virus type 1 model studies. Nucleic Acids Res. **18**:999–1005.

46. **Landau, N. R., M. Warton, and D. R. Littman.** 1988. The envelope glycoprotein of the human immunodeficiency virus binds to the immunoglobulin-like domain of CD4. Nature **334**:159–162.
47. **Lores, P., V. Boucher, C. Mackay, M. Pla, H. Von Boehmer, J. Jami, F. Barre-Sinoussi, and J. C. Weill.** 1992. Expression of human CD4 in transgenic mice does not confer sensitivity to human immunodeficiency virus infection. AIDS Res. Hum. Retrovir. **8**:2063–2071.
48. **Lu, Y. L., P. Spearman, and L. Ratner.** 1993. Human immunodeficiency virus type 1 viral protein R localization in infected cells and virions. J. Virol. **67**:6542–6550.
49. **Maddon, P. J., A. G. Dalgleish, J. S. McDougal, P. R. Clapham, R. A. Weiss, and R. Axel.** 1986. The T4 gene encodes the AIDS virus receptor and is expressed in the immune system and the brain. Cell **47**:333–348.
50. **Maertens, G., P. Cherepanov, W. Pluymers, K. Busschots, E. De Clercq, Z. Debyser, and Y. Engelborghs.** 2003. LEDGF/p75 is essential for nuclear and chromosomal targeting of HIV-1 integrase in human cells. J. Biol. Chem. **278**:33528–33539.
51. **Mancebo, H. S., G. Lee, J. Flygare, J. Tomassini, P. Luu, Y. Zhu, J. Peng, C. Blau, D. Hazuda, D. Price, and O. Flores.** 1997. P-TEFb kinase is required for HIV Tat transcriptional activation in vivo and in vitro. Genes Dev. **11**:2633–2644.
52. **Mariani, R., B. A. Rasala, G. Rutter, K. Wiegers, S. M. Brandt, H. G. Krausslich, and N. R. Landau.** 2001. Mouse-human heterokaryons support efficient human immunodeficiency virus type 1 assembly. J. Virol. **75**:3141–3151.
53. **Mariani, R., G. Rutter, M. E. Harris, T. J. Hope, H. G. Krausslich, and N. R. Landau.** 2000. A block to human immunodeficiency virus type 1 assembly in murine cells. J. Virol. **74**:3859–3870.
54. **Masuda, T., V. Planelles, P. Krogstad, and I. S. Chen.** 1995. Genetic analysis of human immunodeficiency virus type 1 integrase and the U3 att site: unusual phenotype of mutants in the zinc finger-like domain. J. Virol. **69**: 6687–6696.
55. **Miller, D. G., and A. D. Miller.** 1994. A family of retroviruses that utilize related phosphate transporters for cell entry. J. Virol. **68**:8270–8276.
56. **Morikawa, Y., S. Hinata, H. Tomoda, T. Goto, M. Nakai, C. Aizawa, H. Tanaka, and S. Omura.** 1996. Complete inhibition of human immunodeficiency virus Gag myristoylation is necessary for inhibition of particle budding. J. Biol. Chem. **271**:2868–2873.
57. **Neil, S., F. Martin, Y. Ikeda, and M. Collins.** 2001. Postentry restriction to human immunodeficiency virus-based vector transduction in human monocytes. J. Virol. **75**:5448–5456.
58. **Newstein, M., E. J. Stanbridge, G. Casey, and P. R. Shank.** 1990. Human chromosome 12 encodes a species-specific factor which increases human immunodeficiency virus type 1 tat-mediated trans activation in rodent cells. J. Virol. **64**:4565–4567.
59. **Nisole, S., and A. Saib.** 2004. Early steps of retrovirus replicative cycle. Retrovirology **1**:9.
60. **Nisole, S., J. P. Stoye, and A. Saib.** 2005. TRIM family proteins: retroviral restriction and antiviral defence. Nat. Rev. Microbiol. **3**:799–808.
61. **Nomura, H., B. W. Nielsen, and K. Matsushima.** 1993. Molecular cloning of cDNAs encoding a LD78 receptor and putative leukocyte chemotactic peptide receptors. Int. Immunol. **5**:1239–1249.
62. **Ory, D. S., B. A. Neugeboren, and R. C. Mulligan.** 1996. A stable human-derived packaging cell line for production of high titer retrovirus/vesicular stomatitis virus G pseudotypes. Proc. Natl. Acad. Sci. USA **93**:11400–11406.
63. **Petit, C., O. Schwartz, and F. Mammano.** 2000. The karyophilic properties of human immunodeficiency virus type 1 integrase are not required for nuclear import of proviral DNA. J. Virol. **74**:7119–7126.
64. **Piller, S. C., L. Caly, and D. A. Jans.** 2003. Nuclear import of the pre-integration complex (PIC): the Achilles heel of HIV? Curr. Drug Targets **4**:409–429.
65. **Planelles, V., A. Haislip, E. S. Withers-Ward, S. A. Stewart, Y. Xie, N. P. Shah, and I. S. Chen.** 1995. A new reporter system for detection of retroviral infection. Gene Ther. **2**:369–376.
66. **Pluymers, W., P. Cherepanov, D. Schols, E. De Clercq, and Z. Debyser.** 1999. Nuclear localization of human immunodeficiency virus type 1 integrase expressed as a fusion protein with green fluorescent protein. Virology **258**:327–332.
67. **Pollard, V. W., and M. H. Malim.** 1998. The HIV-1 Rev protein. Annu. Rev. Microbiol. **52**:491–532.
68. **Popov, S., M. Rexach, G. Zybarth, N. Reiling, M. A. Lee, L. Ratner, C. M. Lane, M. S. Moore, G. Blobel, and M. Bukrinsky.** 1998. Viral protein R regulates nuclear import of the HIV-1 pre-integration complex. EMBO J. **17**:909–917.
69. **Sakai, H., R. Shibata, J. Sakuragi, S. Sakuragi, M. Kawamura, and A. Adachi.** 1993. Cell-dependent requirement of human immunodeficiency virus type 1 Vif protein for maturation of virus particles. J. Virol. **67**:1663–1666.
70. **Sawada, S., K. Gowrishankar, R. Kitamura, M. Suzuki, G. Suzuki, S. Tahara, and A. Koito.** 1998. Disturbed CD4+ T cell homeostasis and in vitro HIV-1 susceptibility in transgenic mice expressing T cell line-tropic HIV-1 receptors. J. Exp. Med. **187**:1439–1449.
71. **Sherman, M. P., and W. C. Greene.** 2002. Slipping through the door: HIV entry into the nucleus. Microbes Infect. **4**:67–73.
72. **Stremlau, M., C. M. Owens, M. J. Perron, M. Kiessling, P. Autissier, and J. Sodroski.** 2004. The cytoplasmic body component TRIM5alpha restricts HIV-1 infection in Old World monkeys. Nature **427**:848–853.
73. **Suzuki, Y., N. Misawa, C. Sato, H. Ebina, T. Masuda, N. Yamamoto, and Y. Koyanagi.** 2003. Quantitative analysis of human immunodeficiency virus type 1 DNA dynamics by real-time PCR: integration efficiency in stimulated and unstimulated peripheral blood mononuclear cells. Virus Genes **27**:177–188.
74. **Tanaka, J., H. Ozaki, J. Yasuda, R. Horai, Y. Tagawa, M. Asano, S. Saijo, M. Imai, K. Sekikawa, M. Kopf, and Y. Iwakura.** 2000. Lipopolysaccharide-induced HIV-1 expression in transgenic mice is mediated by tumor necrosis factor-alpha and interleukin-1, but not by interferon-gamma nor interleukin-6. AIDS **14**:1299–1307.
75. **Tsuruo, T., T. Yamori, K. Naganuma, S. Tsukagoshi, and Y. Sakurai.** 1983. Characterization of metastatic clones derived from a metastatic variant of mouse colon adenocarcinoma 26. Cancer Res. **43**:5437–5442.
76. **Tsurutani, N., M. Kubo, Y. Maeda, T. Ohashi, N. Yamamoto, M. Kannagi, and T. Masuda.** 2000. Identification of critical amino acid residues in human immunodeficiency virus type 1 IN required for efficient proviral DNA formation at steps prior to integration in dividing and nondividing cells. J. Virol. **74**:4795–4806.
77. **van Maanen, M., and R. E. Sutton.** 2003. Rodent models for HIV-1 infection and disease. Curr. HIV Res. **1**:121–130.
78. **Wei, P., M. E. Garber, S. M. Fang, W. H. Fischer, and K. A. Jones.** 1998. A novel CDK9-associated C-type cyclin interacts directly with HIV-1 Tat and mediates its high-affinity, loop-specific binding to TAR RNA. Cell **92**:451–462.
79. **Yang, W. K., J. O. Kiggans, D. M. Yang, C. Y. Ou, R. W. Tennant, A. Brown, and R. H. Bassin.** 1980. Synthesis and circularization of N- and B-tropic retroviral DNA Fv-1 permissive and restrictive mouse cells. Proc. Natl. Acad. Sci. USA **77**:2994–2998.
80. **Yasuda, J., T. Miyao, M. Kamata, Y. Aida, and Y. Iwakura.** 2001. T cell apoptosis causes peripheral T cell depletion in mice transgenic for the HIV-1 vpr gene. Virology **285**:181–192.
81. **Zack, J. A., S. J. Arrigo, S. R. Weitsman, A. S. Go, A. Haislip, and I. S. Chen.** 1990. HIV-1 entry into quiescent primary lymphocytes: molecular analysis reveals a labile, latent viral structure. Cell **61**:213–222.
82. **Zennou, V., C. Petit, D. Guetard, U. Nerhbass, L. Montagnier, and P. Charneau.** 2000. HIV-1 genome nuclear import is mediated by a central DNA flap. Cell **101**:173–185.
83. **Zheng, Y. H., H. F. Yu, and B. M. Peterlin.** 2003. Human p32 protein relieves a post-transcriptional block to HIV replication in murine cells. Nat. Cell Biol. **5**:611–618.

Hematopoietic stem cell–engrafted NOD/SCID/IL2Rγ^{null} mice develop human lymphoid systems and induce long-lasting HIV-1 infection with specific humoral immune responses

Satoru Watanabe,[1] Kazuo Terashima,[2] Shinrai Ohta,[3] Shigeo Horibata,[3] Misako Yajima,[4] Yoko Shiozawa,[1] M. Zahidunnabi Dewan,[2,3] Zhong Yu,[2] Mamoru Ito,[5] Tomohiro Morio,[6] Norio Shimizu,[1] Mitsuo Honda,[3] and Naoki Yamamoto[2,3]

[1]Department of Virology, Division of Medical Science, Medical Research Institute, Tokyo Medical and Dental University, Japan; [2]Department of Molecular Virology, Graduate School of Medicine, Tokyo Medical and Dental University, Japan; [3]AIDS Research Center, National Institute of Infectious Diseases, Tokyo, Japan; [4]Department of Infectious Diseases, National Research Institute for Child Health and Development, Tokyo, Japan; [5]Central Institute for Experimental Animals, Kanagawa, Japan; and [6]Department of Pediatrics and Developmental Biology, Graduate School of Medicine, Tokyo Medical and Dental University, Japan

Critical to the development of an effective HIV/AIDS model is the production of an animal model that reproduces long-lasting active replication of HIV-1 followed by elicitation of virus-specific immune responses. In this study, we constructed humanized nonobese diabetic/severe combined immunodeficiency (NOD/SCID)/interleukin-2 receptor γ-chain knockout (IL2Rγ^{null}) (hNOG) mice by transplanting human cord blood–derived hematopoietic stem cells that eventually developed into human B cells, T cells, and other monocytes/macrophages and dendritic cells associated with the generation of lymphoid follicle–like structures in lymphoid tissues. Expressions of CXCR4 and CCR5 antigens were recognized on CD4$^+$ cells in peripheral blood, the spleen, and bone marrow, while CCR5 was not detected on thymic CD4$^+$ T cells. The hNOG mice showed marked, long-lasting viremia after infection with both CCR5- and CXCR4-tropic HIV-1 isolates for more than the 40 days examined, with R5 virus–infected animals showing high levels of HIV-DNA copies in the spleen and bone marrow, and X4 virus–infected animals showing high levels of HIV-DNA copies in the thymus and spleen. Furthermore, we detected both anti–HIV-1 Env gp120– and Gag p24–specific antibodies in animals showing a high rate of viral infection. Thus, the hNOG mice mirror human systemic HIV infection by developing specific antibodies, suggesting that they may have potential as an HIV/AIDS animal model for the study of HIV pathogenesis and immune responses. (Blood. 2007; 109:212-218)

Introduction

Current animal models for either human immunodeficiency virus type 1 (HIV-1) or simian immunodeficiency virus (SIV) suffer from the lack of a system precisely mirroring human HIV infection and the progression to disease state.[1] In current animal models with HIV infection, such as chimpanzees, animals do not develop AIDS.[1] Past animal models for HIV infection have relied on humanized severe combined immunodeficiency (hSCID) mice models to study prospective anti-HIV drugs and vaccines. SCID-hu (Thy/Liv) mice, engrafted with human fetal thymus and liver tissue in the renal subcapsular region, were first reported as the small-animal model.[2] Because human T cells are generated within the engrafted thymus, this model has been used for the study of thymopoiesis[3-6] and hematopoiesis[7,8] under the burden of HIV-1 infection. However, this model allows for a limited systemic HIV-1 infection, which is restricted mainly to the engrafted thymus. Another HIV mouse model, hu-PBL–SCID mice engrafted with human peripheral blood mononuclear cells (PBMCs),[9] has been actively used as a tool in developing antiretroviral therapy.[9-11] However, the infection persists for only a short time in association with rapid loss of CD4$^+$ T cells because there is no active hematopoiesis or thymopoiesis.[9,12,13] Furthermore, these mouse models fail to mirror certain key aspects of the human immune response, lacking normal lymphoid tissue and functional human antigen-presenting cells such as dendritic cells (DCs).[14] Thus, although these mouse models are valuable as animal models for HIV infection, the development of a mouse model more analogous to human HIV infection is needed if we are to better understand HIV pathogenesis and develop successful anti-HIV therapies and preventive vaccines.

To solve the difficult issue about the development of an ideal HIV mouse model, we initially selected a humanized nonobese diabetic (NOD)/SCID interleukin-2 receptor (IL-2R) γ-chain knockout (NOG) mouse[15] as a model animal because it has been suggested that multilineage cells, including human T, B, and natural killer (NK) cells, differentiate in these mice when given transplants of human CD34$^+$ hematopoietic stem cells.[16-18] In the current study, we further reveal the kinetics of differentiation of human B and T cells, monocytes/macrophages, and DCs in the mice that received transplants, and we characterize the animals by infection with both CCR5 (R5)– and CXCR4 (X4)-tropic HIV strains. Since our hNOG mice show stable and systemic infection of both R5- and X4-tropic HIV for more than

Submitted April 20, 2006; accepted August 12, 2006. Prepublished online as *Blood* First Edition Paper, September 5, 2006; DOI 10.1182/blood-2006-04-017681.

The publication costs of this article were defrayed in part by page charge payment. Therefore, and solely to indicate this fact, this article is hereby marked "advertisement" in accordance with 18 USC section 1734.

the 40 days studied, and HIV-specific antibodies are detectable in the animals with high plasma viral loads and HIV-DNA copy numbers, we also discuss the suitability of HIV-hNOG mice as an animal model for HIV-1 infection.

Materials and methods

Transplantation of human CB-derived hematopoietic stem cells in NOG mice

Human cord blood (CB) was obtained from Saiseikai Central hospital (Minato-ku, Tokyo, Japan) and Tokyo Cord Blood Bank (Katsushika-ku, Tokyo, Japan) after obtaining informed consent. All research on human subjects was approved by the Institutional Review Board of each institution participating in the project. CB mononuclear cells were separated by Ficoll-Hypaque density gradient. $CD34^+$ hematopoietic stem cells were isolated using a magnetic-activated cell sorting (MACS) Direct CD34 Progenitor Cell Isolation Kit (Miltenyi Biotec, Bergisch Gladbach, Germany) according to the manufacturer's instructions. More than 95% of $CD34^+$ cells were positively selected after 2 time-enrichment manipulations. Cells were either immediately used for the transplantation or frozen until use. NOG mice were obtained from the Central Institute for Experimental Animals (Kawasaki, Japan) and maintained under specific pathogen–free (SPF) conditions in the animal facility of the National Institute of Infectious Diseases (NIID; Tokyo, Japan). Mice used in these studies were free of known pathogenic viruses, herpes viruses, bacteria, and parasites. They were housed in accordance with the Guidelines for Animal Experimentation of the Japanese Association for Laboratory Animal Science (1987) under the Japanese Law Concerning the Protection and Management of Animals, and were maintained in accordance with the guidelines set forth by the Institutional Animal Care and Use Committee of NIID, Japan. Once approved by the Institutional Committee for Biosafety Level 3 experiments, these studies were conducted at the Animal Center, NIID, Japan, in accordance with the requirements specifically stated in the laboratory biosafety manual of the World Health Organization. Female mice (6 to 10 weeks old) were irradiated (300 cGy) and 1×10^4 to 1.2×10^5 $CD34^+$ cells were intravenously injected within 12 hours.

Flow cytometry

The purity of CB-derived $CD34^+$ cells after separation was evaluated by double staining with FITC-conjugated anti–human CD45 (J.33) and PE-conjugated anti–human CD34 (Class III 581) (all from Beckman Coulter, Fullerton, CA). After transplantation (1-7 months), peripheral blood, spleens, bone marrow (BM), and thymi were collected for flow cytometric analysis following staining with the following monoclonal antibodies (mAbs): FITC-conjugated anti–human CD45 (J.33), CD3 (UCHT1), CD4 (13B8.2), CD19 (J4.119), CD45RO (UCHL1) (all from Beckman Coulter), and CCR5 (2D7; BD Pharmingen, San Diego, CA); PE-conjugated anti–human CD4 (13B8.2), CD8 (B9.11), CD19 (J4.119), CD45RA (ALB11) (all from Beckman Coulter), and CXCR4 (44717; R&D Systems, Minneapolis, MN); anti–mouse CD45 (YW62.3; Beckman Coulter); ECD-conjugated anti–human CD45 (J.33; Beckman Coulter); and PC5-conjugated anti–human CD8 (T8) and CD14 (Rm052) (all from Beckman Coulter). Flow cytometric analysis was conducted by 2- or 4-color staining using an EpicsXL (Beckman Coulter).

Immunohistochemistry

Organs were snap-frozen following embedding in OCT compound (Sakura Finetechnical, Tokyo, Japan). Frozen sections were air-dried and fixed in acetone. HIV-1–infected organs were fixed in 4% paraformaldehyde and embedded in OCT compound following immersion in gradient sucrose (5%-30%). Fixed samples were stained with the following mAbs: anti–human CD45 (1.22/4014; Nichirei, Tokyo, Japan), CD3 (UCHT1; DAKO, Glostrup, Denmark), CD20 (L26; DAKO), CD68 (KP1; DAKO), CD205 (MG38; eBioscience, San Diego, CA), and DRC-1 (R4/23; DAKO) for follicular dendritic cells (FDCs); anti–mouse FDC-M1 (BD Pharmingen) for murine FDCs; and HIV-1 Gag p24 (DAKO) for detection of infected cells. Biotin-labeled goat $F(ab')_2$ anti–mouse immunoglobulin (Ig; ICN Biomedicals, Aurora, OH)– or biotin-labeled mouse $F(ab')_2$ anti–rat IgG (Jackson ImmunoResearch Laboratories, West Grove, PA) was used as the secondary antibody. Samples were treated with alkaline phosphatase (AP) or horseradish peroxidase (HRP)–streptavidin conjugate (ZYMED Laboratories Inc, San Francisco, CA). BCIP/NBT, DAB, or AEC (all from DAKO) was used for the visualization. Photographs were taken by light microscopy (Leica DMRA; Leica Microsystems Wetzlar, Wetzlar, Germany) using Leica HC PLAN APO lenses (10×/0.40 NA PH1). Leica Q550 was used for image processing.

Measurement of human Igs in mice plasma

Plasma concentrations of human IgM, IgG, and IgA in NOG mice that received transplants of human stem cells were determined by conventional human Ig quantitation assay at BML Inc (Tokyo, Japan).

Cells and viruses

Human embryonic kidney 293T cells and monkey kidney COS7 cells were cultured in RPMI 1640 supplemented with 10% fetal bovine serum (FBS) and antibiotics. The 293T cells and COS7 cells were used for transfection of DNA plasmids containing HIV-1_{JRCSF} and simian/human immunodeficiency virus (SHIV)–C2/1, respectively. The SHIV-C2/1 strain contains the *env* gene of pathogenic HIV-1 strain 89.6.[19] Cell-free supernatant was collected and stored at −80°C before use. A primary clinical isolate, HIV-1_{MNp}, was kindly provided by Dr J. Sullivan of the University of Massachusetts Medical School (Worcester, MA). PBMCs isolated from HIV-1–seronegative individuals were cultured in RPMI 1640 supplemented with 10% FBS and antibiotics with 5 μg of phytohemagglutinin (PHA)/mL for 3 or 7 days (PHA-PBMCs). HIV-1_{MNp} was propagated in PHA-PBMCs, and cell-free virus stocks were stored at −80°C.

The 50% tissue-culture infectious dose ($TCID_{50}$) was determined using PHA-PBMCs and the endpoint dilution method. A 4-fold series of dilution was prepared from the virus stock, and then cells were mixed and cultured for 7 days for X4–HIV-1 and 14 days for R5–HIV-1 in RPMI 1640 supplemented with 20% FBS and antibiotics. The endpoints were determined by screening for the p24 antigen using Lumipulse (Fujirevio, Tokyo, Japan).

HIV-1 infection

All procedures for the infection and maintenance of NOG mice were performed in Biosafety Level 3 facilities at NIID under standard caging conditions. On days 102 to 132 after stem cell transplantation, 16 mice were inoculated intravenously with R5-tropic HIV-1_{JRCSF} (65 000 $TCID_{50}$) or X4-tropic SHIV-C2/1 (50 000 $TCID_{50}$). On days 18 to 43 after inoculation, plasma was collected to determine HIV-RNA copy numbers, and spleen cells were prepared as single-cell suspensions to analyze the CD4/CD8 ratio using flow cytometry. A number (14) of other mice were inoculated intravenously with R5-tropic HIV-1_{JRCSF} (200 or 65 000 $TCID_{50}$) or X4-tropic HIV-1_{MNp} (180 or 20 000 $TCID_{50}$) on days 126 to 146 after transplantation. On days 18 to 40 after inoculation, plasma was collected for the determination of HIV-RNA copy numbers, and single-cell suspensions of the spleen, BM, and thymus were prepared for HIV-DNA measurement. The CD4/CD8 ratio in the spleen and percentages of human $CD45^+$ cells in organs were analyzed using flow cytometry.

Virologic analysis

Plasma viral RNA copy numbers were measured using a real-time quantification assay based on the TaqMan system (Applied Biosystems, Foster City, CA). Plasma viral RNA was extracted and purified using a QIAamp Viral RNA Mini Kit (Qiagen, Valencia, CA). The RNA was subjected to reverse transcription (RT) and amplification using a TaqMan One-Step RT–polymerase chain reaction (PCR) Master Mix Reagents Kit (PE Biosystems, Foster City, CA) with HIV-1 gag consensus primers

(forward, 5′-GGACATCAAGCAGCCATGCAA-3′; and reverse, 5′-TGCTATGTCACTTCCCCTTGG-3′) and an HIV-1 gag consensus TaqMan probe (FAM-5′-ACCATCAATGAGGAAGCTGCAGAA-3′-TAMRA). For SHIV-C2/1 analysis, primers (forward, 5′-AATGCAGAGCCCCAAGAAGAC-3′; and reverse, 5′-GGACCAAGGCCTAAAAAACCC-3′) and a TaqMan probe (FAM-5′-ACCATGTTATGGCCAAATGCCCAGAC-3′-TAMRA) were designed for targeting the SIVmac239 gag region.[20] Probed products were quantitatively monitored by their fluorescence intensity with the ABI7300 Real-Time PCR system (PE Biosystems). To obtain control RNA for quantification, HIV-1 gag RNA and SIVmac239 gag RNA were synthesized using T7 RNA polymerase and pKS460. Viral DNA was extracted and purified using a QIAamp DNA Mini Kit (Qiagen). Determination of HIV-1 DNA copy numbers was performed by real-time PCR assay with TaqMan Master mixture (PE Biosystems). Primers (forward, 5′-GGCTAACTAGGGAACCCACTG-3′; and reverse, 5′-CTGCTAGAGATTTTCCACACT-3′) and probes (FAM-5′-TAGTGTGTGCCCGTCTGTTGTGTGAC-3′-TAMRA) were designed for targeting the HIV-1 long terminal repeat region, R/U5. The viral DNA was quantified using LightCycler (Roche Diagnostics, Almere, The Netherlands). Viral RNA and DNA were calculated based on the standard curve of control RNA and DNA. All assays were carried out in duplicate.

HIV-antigen ELISA

Levels of anti–HIV-1 Igs against recombinant HIV-1_{IIIB} Env gp120, recombinant HIV-1_{MN} Env gp120, and recombinant HIV-1_{IIIB} Gag p24 (all from ImmunoDiagnostics Inc, Woburn, MA) in plasma from HIV-1–infected and –uninfected control mice were determined using a standard enzyme-linked immunosorbent assay (ELISA). Microplates (96-well) were coated overnight with 200 ng/well antigens, and plasma diluted 1:20, 1:60, and 1:180 with PBS were incubated for 1 hour. AP-labeled anti–human Igs (γ, α, and μ; Sigma-Aldrich, St Louis, MO) were used as secondary antibodies. P-nitrophenylphosphate (pNPP) Solution (WAKO Chemical USA, Richmond, VA) was used for the visualization. The enzyme reaction was stopped by addition of 0.1 M NaOH and read at 405 nm. All assays were carried out in triplicate.

Statistical analysis

Data were expressed as the mean value ± standard deviation (SD). Significant differences between data groups were determined by 2-sample Student *t* test analysis. A *P* value less than .05 was considered significant.

Results

Reconstitution of human lymphoid systems in hNOG mice

The initial studies describing the construction of humanized SCID mice used the human PBMC for infection of immunodeficiency viruses.[9,12,21] However, these hu-PBL-SCID mice showed a partial infection to the R5 virus and a relatively limited period of viral replication. To construct a more suitable mouse model mimicking HIV-1 infection in humans, we selected human CB stem cells as a transplant for NOG mice. NOG mice were inoculated intravenously with human CD34$^+$ hematopoietic stem cells, and their development of human lymphoid systems were then monitored. After transplantation (2 months), human CD45$^+$ leukocytes were recognized in both PB and the spleen, but most of the cells were human B cells (Figure 1A). Human T cells began to be recognized clearly in PB and the spleen 4 months after transplantation (Figure 1B) and gradually increased in level, as did human B cells (Figure 1C).

In Figure 1D, we summarized percentages of human CD3$^+$ T cells in human CD45$^+$ cells from 38 mice from 39 to 213 days after transplantation. Human CD3$^+$ T cells clearly increased 100 days after transplantation in both PB and the spleen. After transplantation (4 months), human CD3$^+$ T cells in the spleen preferably expressed CD45RA rather than CD45RO (70.8% ± 13.4% and 27.3% ± 38.8% in CD3$^+$ T cells, respectively; n = 5; Figure 1E), demonstrating that most of the T cells were in a naive state. In addition, plasma taken from 5 mice 113 to 143 days after transplantation showed that all mice produced human IgM, with concentrations ranging from 0.025 to 0.5 g/L, and that human IgG and IgA was also detected in some of the mice (ranges, 0.015-0.18 g/L and 0.003-0.012 g/L, respectively) (data not shown).

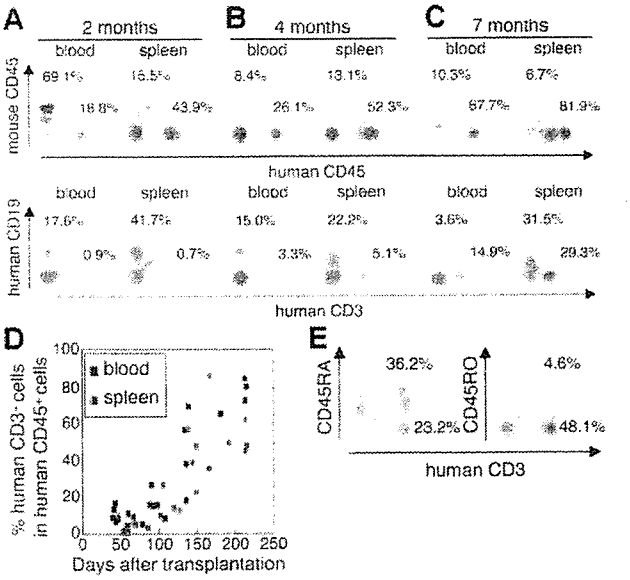

Figure 1. Flow cytometric analysis of human T cells in the peripheral blood and spleen in NOG mice given intravenous transplants of human CB-derived CD34$^+$ cells. (A-C) Representative profiles of the mice 2 months (A), 4 months (B), and 7 months (C) after transplantation. The ratio of human to murine CD45$^+$ cells and that of human CD3$^+$ to CD19$^+$ cells show an incremental increase in human CD45$^+$ cells and human CD3$^+$ cells from 2 to 7 months. (D) Change of net percentages of human CD3$^+$ T cells among human CD45$^+$ cells in peripheral blood and the spleen from 38 mice 39 to 213 days after transplantation. (E) CD45RA is more efficiently expressed than CD45RO on human CD3$^+$ T cells in spleen. A gate was set on the human CD45$^+$ population. The fluorescence-activated cell sorting (FACS) profile is representative of 1 in a group of 5 mice.

By 7 months after transplantation, human CD45$^+$ leukocytes comprised more than 80% to 90% of mononuclear cells in the spleen (Figure 1C), and most of the mice showed symptoms of a wasting condition and a hunched back. Based upon these results, we determined that the suitable period for HIV inoculation would be 4 to 5 months after transplantation.

Formation of lymphoid structures, including monocytes/macrophages, DCs, and FDCs

Next, using the hNOG mice at 4 months after transplantation, we investigated lymphoid structure formation and the development of human monocytes, macrophages, DCs, and FDCs, which are very important factors not only for elicitation of immune responses against foreign antigens, but also for the spread of HIV-1 infection in a body.[22-24] Human CD14$^+$ monocytes were detected in PB, the spleen, and BM using flow cytometry (Figure 2A). During immunohistochemical analysis, human CD45$^+$ leukocytes gathered in a form of follicle-like structures (FLSs) at the end of the central artery in the spleen (Figure 2B). From a serial section of the same region (Figure 2B-G), these structures consisted mainly of human CD20$^+$ B cells (Figure 2C) admixed with a small number of human CD3$^+$ T cells (Figure 2D). Hardly any human FDCs positive for DRC-1 were detected (data not shown), whereas a

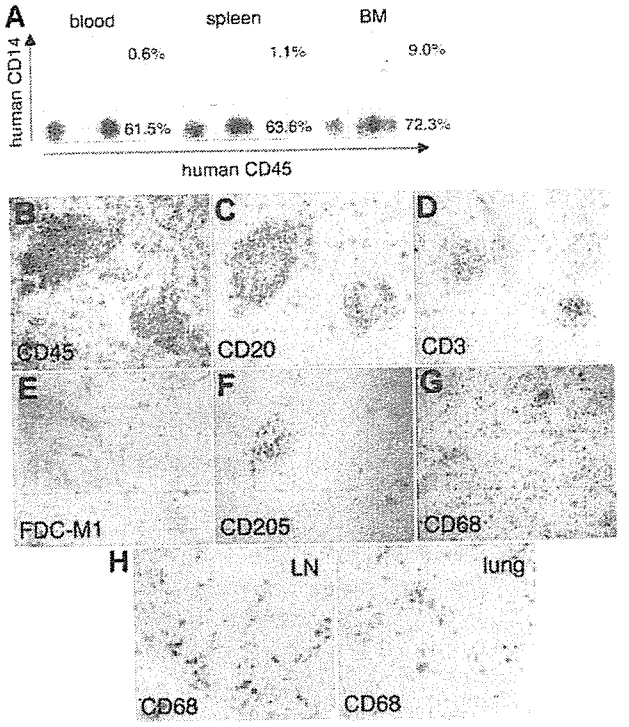

Figure 2. Flow cytometric analysis and immunohistochemical analysis of the expression of myelomonocytic markers in hNOG mice 4 months after transplantation. (A) Human CD14$^+$ monocytes/macrophages are recognized in peripheral blood, the spleen, and BM. (B-G) Immunohistochemical findings from serially sectioned spleen for the expressions of human CD45 (B), human CD20 (C), human CD3 (D), murine FDC (E), human CD205 (F), and human CD68 (G). (H) Human CD68$^+$ macrophages are also detected in the medulla of the LN and lung. Visualization was performed with BCIP (B-D, F-G), DAB (E), and AEC (H). Original magnification, ×100.

loose network of murine FDCs positive for FDC-M1 was recognized in the distal portion of the FLSs (Figure 2E). Human CD205$^+$ DCs were predominantly detected in a cluster form within the FLSs (Figure 2F), while human CD68$^+$ macrophages were scattered throughout the spleen (Figure 2G). Many human CD68$^+$ macrophages were also observed in various other organs, including the lymph nodes (LNs) and the lungs (Figure 2H).

Expression of HIV-1 coreceptors on CD4$^+$ cells in various tissues

Since the development of lymphoid tissues was recognized in hNOG mice, we focused on the expressions of HIV-1 coreceptors CXCR4 and CCR5 on human CD4$^+$ cells in these tissues. CXCR4 antigen was expressed in 36.5% ± 4.2% (n = 4) of the CD4$^+$ cells in PB (Figure 3A) and 78.1% ± 17.1% (n = 5) in the spleen (Figure 3B). CCR5$^+$ cells were detected in 15.5% ± 1.8% (n = 4) of CD4$^+$ cells in PB and 28.6% ± 12.6% (n = 5) in the spleen (Figure 3A-B). In the thymus, CD4$^+$CD8$^+$ thymocytes existed in 82.9% ± 4.4% (n = 5) as well as small numbers of CD4$^+$CD8$^-$ cells (6.4% ± 2.4%; n = 5) and CD4$^-$CD8$^+$ cells (7.7% ± 3.0%; n = 5), with the CXCR4 antigen expressed in 50.1% ± 4.5% (n = 5) of CD4$^+$ cells, while, as with normal human thymocytes,[25] CCR5$^+$ cells were almost undetectable, with less than 1% (0.6% ± 0.1%; n = 5) (Figure 3C). Human CD3$^+$ T cells and CD14$^+$ monocytes in BM were detected only in 3.2% ± 2.1% and 5.8% ± 3.8%, respectively, while CD4$^+$ cells were recognized in 18.1% ± 6.5%, with many expressing both CXCR4 (75.0% ± 23.1%) and CCR5 (81.3% ± 6.6%; n = 5; Figure 3D). Thus, distributions of HIV-1 coreceptor–positive cells in these lymphoid tissues suggest that the hNOG mice allow for sufficient development of human cells to make the study of HIV-1 pathogenesis possible.

Both R5- and X4-tropic HIVs efficiently infect and replicate in hNOG mice

In our preliminary study, using low and high doses of challenge virus, no viral infection was detected in any of the virus-inoculated hNOG mice at 7 days after infection, while some showed detectable plasma viral loads at 14 days (data not shown). Then, we prepared 16 hNOG mice that received transplants of stem cells and inoculated them with a high dose of R5-tropic HIV-1_{JRCSF} (65 000 $TCID_{50}$) and X4-tropic SHIV-C2/1 (50 000 $TCID_{50}$) intravenously through the tail vein at 102 to 132 days after transplantation. Upon HIV-1_{JRCSF} infection, viral copy numbers in plasma rose to a level of 1.6×10^5 to 5.8×10^5 copies/mL (n = 4) on day 33 and 2.0×10^5 to 4.7×10^5 copies/mL on day 43 (n = 4) (Figure 4A). Moreover, for SHIV-C2/1 infection, viral copy numbers in plasma were 1.6×10^3 to 3.2×10^5 copies/mL on day 18 (n = 4) and reached 5.4×10^4 to 1.1×10^5 copies/mL on day 42 (n = 4; Figure 4B). In these mice, no significant decline in the CD4/CD8 ratio was observed throughout entire period of follow-up for the R5-tropic virus infection, while CD4$^+$ cell decline was detected for the X4-tropic virus infection on day 42 after infection ($P = .044$) but not on day 18 after infection (Figure 4C). Four mice that did not receive transplants of human stem cells showed no detectable levels of plasma viral load (less than 500 copies/mL) following HIV/SHIV inoculation (data not shown).

To confirm HIV infection, we used immunohistochemistry to detect the presence of the p24 antigen of the HIV-1 Gag protein in various tissues of mice showing viremia. p24$^+$ cells were clearly identified in the spleen, LN, and lungs (Figure 4D), which include macrophage-like cells.

Different distributions of R5- and X4-tropic viruses in lymphoid tissues

A number of mice (14) were further analyzed for HIV-1 infection on days 126 to 146 after transplantation with a low dose (200 $TCID_{50}$) or a high dose (65 000 $TCID_{50}$) of R5-tropic HIV-1_{JRCSF} and a low dose (180 $TCID_{50}$) or a high dose (20 000 $TCID_{50}$) of X4-tropic HIV-1_{MNp}. Consequently, 2 of the 4 mice given a low

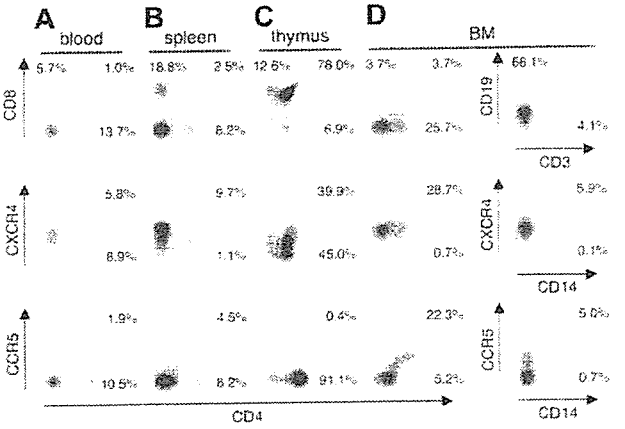

Figure 3. Surface expression of HIV-1 coreceptors on CD4$^+$ cells in various organs of mice 4 months after transplantation. A representative FACS profile of human CXCR4 and CCR5 on CD4$^+$ cells shows the existence of CXCR4$^+$CD4$^+$ and CCR5$^+$CD4$^+$ cells in blood (A), spleen (B), and BM (D), but no CCR5$^+$CD4$^+$ cells in the thymus (C). BM results show that many CD4$^+$ cells are neither CD3$^+$ T cells nor CD14$^+$ monocytes. A gate was set on the human CD45$^+$ population.

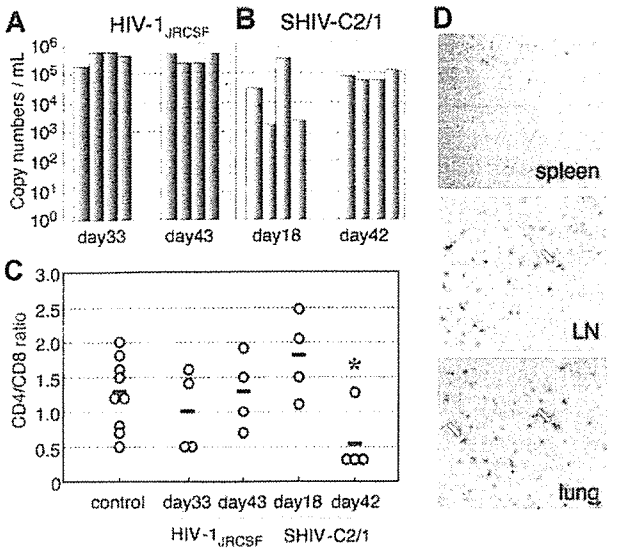

Figure 4. The numbers of RNA viral copies in plasma, CD4+/CD8+ T-cell ratios in the spleen, and p24 detection in the immunohistochemistry of HIV/SHIV-infected mice. (A) Viral copy numbers of 8 mice inoculated with a high infectious dose of HIV-1_{JRCSF} (65 000 $TCID_{50}$) and killed on days 33 and 43 after inoculation. (B) Viral copy numbers of 8 mice inoculated with a high infectious dose of SHIV-C2/1 (50 000 $TCID_{50}$) and killed on days 18 and 42 after inoculation. Note that all the mice showed high levels of viremia that lasted more than 40 days after inoculation. (C) CD4/CD8 cell ratios in the spleens of 16 infected mice and 9 uninfected control mice. Control mice were not inoculated with HIV/SHIV and were killed on days 105 to 166 after stem cell transplantation. There was no significant rapid loss of $CD4^+$ cells in HIV-1_{JRCSF}–infected mice, while a decline of the CD4/CD8 ratio was detected in SHIV-C2/1–infected mice on day 42 after infection compared with uninfected control mice (*$P < .05$). The short bars indicate the means of each group. (D) $P24^+$ cells are clearly observed in the spleen, LNs, and lungs. Arrow indicates p24 positive for macrophage-like cells. Original magnification, ×100.

dose of HIV-1_{JRCSF} and 2 of the 3 mice given a low dose of HIV-1_{MNp} were successfully infected (Table 1), suggesting that each dose represents an approximately 50% infectious dose of HIV for hNOG mice. High HIV-DNA copy numbers were mainly detected in the spleen and BM of the HIV-1_{JRCSF} –infected mice, and in the thymus and spleen of the HIV-1_{MNp}–infected mice, while their BM showed lower copy numbers (Table 1).

Generation of HIV-specific antibodies in hNOG mice at a high multiplicity of infection

We then tested for generation of human antibodies against HIV-1 from these 14 mice by HIV antigen-specific ELISA. The sera of mice no. 136-3 and no. 157-3 infected with HIV-1_{JRCSF} and HIV-1_{MNp}, respectively, showed significant levels of human antibodies specific for HIV-1_{IIIB}-Env gp120 (Figure 5A), HIV-1_{MN}-Env gp120 (Figure 5B), and HIV-1_{IIIB}-Gag p24 (Figure 5C). In addition, no. 157-4 sera from an HIV-1_{MNp}–infected animal was also weakly positive for their Env and Gag antigens. These animals showed intense plasma viral loads and enhanced proviral DNA copies in the spleen, BM, and thymus (Table 1), suggesting that hNOG mice inoculated with high doses of HIV and showing high rates of viral infection develop HIV-1–specific humoral immune responses that are analogous to those seen in human anti-HIV B-cell responses.

Discussion

Current small-animal models fall short of accurately mirroring human HIV-1 infection and thus have limited usefulness in analyzing the natural course of its progression to the disease state and in developing antiviral countermeasures. Although successful HIV-1 infections in immunodeficiency mice humanized with PBMCs have been reported,[12,13,21] transplanted human cells are soon depleted and do not elicit virus-specific immune responses, shedding little light on pathogenesis and vaccine development. By using NOG mice that received hematopoietic stem cell transplants showing high rates of viral infection, we demonstrated HIV-specific antibody responses and viral infection parameters, including the following: (1) similar levels of susceptibility to both R5- and X4-tropic HIV-1; (2) high levels of viremia stably observed over 40 days; (3) immunohistochemical detection of infected cells in various organs; and (4) a distinct tissue distribution for R5- versus X4-tropic HIV-1s.

Among $CD4^+$ T cells, CXCR4 antigen is primarily expressed on naive and CCR5 on activated or memory cells.[26] hu-PBL-SCID mice become susceptible to R5-tropic HIV-1 strains,[27] since T cells

Table 1. Comparison of viral RNA copies in plasma and HIV-DNA copies in the spleen, BM, and thymus from hNOG mice receiving low- and high-dose viral inoculations

Mouse ID no.	HIV strain	$TCID_{50}$	Time after inoculation, d	RNA viral copies/mL	CD4/CD8 ratio	HIV-DNA copies/10^6 human cells		
						Spleen	BM	Thymus
Low-dose viral inoculation group								
113-1	HIV-1_{JRCSF}	200	18	6 240	1.8	34 177	11 785	3 495
112-2	HIV-1_{JRCSF}	200	18	<500	1.2	< 100	< 100	< 100
113-2	HIV-1_{JRCSF}	200	40	6 177	1.6	25 855	27 920	3 473
112-3	HIV-1_{JRCSF}	200	40	<500	0.9	< 100	< 100	<100
112-4	HIV-1_{MNp}	180	18	72 477	1.3	18 873	100	ND
113-4	HIV-1_{MNp}	180	40	70 667	0.3	4 947	653	32 163
112-1	HIV-1_{MNp}	180	40	<500	0.9	< 100	< 100	< 100
High-dose viral inoculation group								
136-3	HIV-1_{JRCSF}	65 000	25	252 381	0.8	958 871	1 797 600	232 155
136-2	HIV-1_{JRCSF}	65 000	29	50 167	0.7	41 172	54 521	8 600
141-1	HIV-1_{JRCSF}	65 000	30	67 667	2.2	27 735	52 430	429
161-3	HIV-1_{JRCSF}	65 000	30	13 847	0.9	104 466	14 653	111 080
157-3	HIV-1_{MNp}	20 000	31	1 253 925	0.5	41 053	56 802	976 556
157-4	HIV-1_{MNp}	20 000	31	147 973	0.6	3 634	262	40 796
161-6	HIV-1_{MNp}	20 000	31	108 073	1.7	4 991	< 100	3 673

Seven mice inoculated with a low infectious dose of HIV-1_{JRCSF} (200 $TCID_{50}$) or HIV-1_{MNp} (180 $TCID_{50}$), and 7 mice receiving a high infectious dose of HIV-1_{JRCSF} (65 000 $TCID_{50}$) or HIV-1_{MNp} (20 000 $TCID_{50}$) were listed.

ND indicates not done.

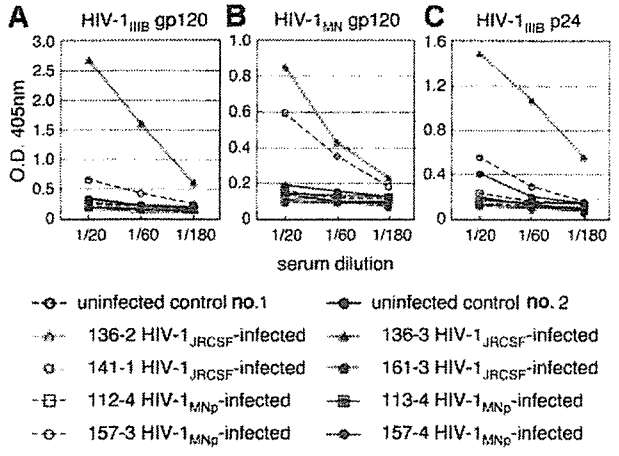

Figure 5. Detection of anti–HIV-1 antibodies from the plasma of HIV-1–infected mice. An ELISA assay was conducted by using plasma from 14 mice inoculated with either HIV-1_{JRCSF} or HIV-1_{MNp}, and from 2 uninfected control mice. Representatives (n = 8) of the 14 HIV-1–inoculated mice, and the 2 uninfected mice, are shown in the panels. Measurements of specific human antibodies for HIV-1_{IIIB} gp120 (A), HIV-1_{MN} gp120 (B), and HIV-1_{IIIB} p24 antigens (C) were shown. Results are expressed as the means from triplicate assays in 3 different experiments.

are initially activated in the xenogenic environment and then become anergic.[14] In contrast, SCID-hu (Thy/Liv) mice are more susceptible to X4 than to R5 strains[6] because HIV-1 infection is restricted mainly to the engrafted thymus that is primarily comprised of immature T cells, suggesting that this model may not be practical overt HIV infection. Our study represents the first attempt to infect NOG mice that received transplants of human hematopoietic stem cells with HIV-1. Very similar infection rates were seen for both R5 and X4 strains in the mouse model. Flow cytometry revealed both $CXCR4^+CD4^+$ and $CCR5^+CD4^+$ cells in PB, the spleen, and BM, but only CXCR4 on thymic $CD4^+$ T cells. It also showed the scattering of human macrophages, known to be susceptible to R5-tropic HIV-1 strains[28,29] and the source of HIV-1.[23,30-32] throughout various organs. $p24^+$ macrophage-like cells were detected in these organs after R5-tropic HIV-1_{JRCSF} infection. These data may help explain the susceptibility of hNOG mice to both R5- and X4-tropic HIV strains and also shed light on the active replenishment of these target cells in mice.

SCID mouse systems have been actively used in the evaluation of anti–HIV-1 drugs.[9,11,21] In most cases, HIV-1 detection levels reach a peak within a month after inoculation and level off, accompanied by $CD4^+$ T-cell depletion.[3,12,13] Although suitable for short-term experiments, it is also true that these models require large numbers of mice because of large variations in infection efficiency. In contrast, very stable infections were noted in our hNOG mice that were inoculated with a high dose of HIVs. They did not show rapid CD4/CD8 decrease in spite of high levels of viremia persisting for more than 40 days. Efficient hematopoiesis and thymopoiesis of human cells probably compensated for the loss of $CD4^+$ T cells, allowing for persistent infection. This capacity of the hNOG mouse system makes it attractive as a model for the long-term evaluation of anti–HIV-1 drugs. In addition to destroying mature blood cells, altered hematopoiesis in BM and the thymus has also been reported to be responsible for immunodeficiency in patients with AIDS.[33,34] To study hematopoietic abnormalities in HIV-1 infection, both SCID-hu (Thy/Liv) mice[8,35,36] and SIV- or SHIV-infected macaque models[20,37-39] have been used. The current hNOG mouse system, in which human cells are efficiently reproduced from stem cells and then settled into hematopoietic organs, offers a promising model for the study of events that occur after infection not only with R5-tropic HIV-1 but also with X4-tropic HIV-1. Indeed, the BM of hNOG mice infected with R5-tropic HIV-1 exhibited exceptionally elevated levels of HIV-DNA copies. On the other hand, the thymus of X4-tropic HIV-1_{MNp}–infected hNOG mice yielded large numbers of HIV-DNA copies, which seemed to correlate with the predominant expression of CXCR4 on the thymocytes. Thus, further observation is essential to address whether AIDS symptoms such as considerable $CD4^+$ T-cell depletion and hematopoietic abnormalities eventually occur in these mice.

It is noteworthy that human antibodies against both HIV-1 Env gp120 and Gag p24 antigens were detected in mice no. 136-3, no. 157-3, and no. 157-4 after exposure to high titers of HIV-1, suggesting that hNOG mice have the ability to respond to HIV-1 antigens. This encourages us to develop antibody-based HIV vaccine candidates, although additional modifications are required for the stable induction of immune responses. Importantly, since the seroconverted mice showed high viremia and high numbers of proviral DNA copies in the spleen, BM, and thymus, abundant viral production may stimulate human B-cell responses against HIV-1 and generate specific antibodies. These mice showed little or no detectable human IgG against HIV-1, as determined by Western blot analysis (data not shown), suggesting that very low levels of class-switching occurred in these mice, though further study is required.

In addition to the humoral immune responses, the induction of primary T-cell responses is critical for the study of HIV-specific immune responses and pathogenesis, as well as for vaccine development. Although we did not demonstrate the T-cell ability to respond to virus antigens, human T cells from the spleen proliferated when stimulated with anti–human CD3 antibodies (data not shown), indicating that the human T cells in the NOG mice that received transplants of hematopoietic stem cells are capable of responding to T-cell receptor–mediated signals and are expected to be able to elicit primary antigen-specific immune responses against foreign antigens. To address whether the specific T-cell responses may be induced will be one of the important studies.

In conclusion, the NOG mice that received transplants of human hematopoietic stem cells successfully achieved systemic and persistent infection with both R5-tropic and X4-tropic HIV-1, and generated humoral immune responses against HIV-1. These capacities of the hNOG mouse model may be very attractive for the study of HIV pathogenesis and humoral immune responses induced by HIV vaccine candidates.

Acknowledgments

We thank Yuetsu Tanaka of the University of Ryukyus, Tetsutaro Sata of NIID, and Shuzo Matsushita of Kumamoto University for their kind provision of mAbs to HIV-1, as well as Yukoku Tamaoka of Saiseikai Central Hospital, Toshio Akashi of Kumakiri Obstetric and Gynecologic Clinic, and Hideo Mugishima of Nihon University School of Medicine for their provision of umbilical cord blood. We also would like to express our gratitude to Ken Watanabe and Hideko Ogata of Tokyo Medical and Dental University for their skillful technical support.

This work was supported by grants from Research on Health Sciences focusing on Drug Innovation, the Japan Health Sciences Foundation.

Authorship

Contributions: S.W., K.T., N.S., M.H., and N.Y. designed the study; S.W., K.T., S.O., S.H., M.Y., Y.S., M.Z.D., and Z.Y. carried out the research; M.I. contributed live mice; S.W., K.T., and T.M. analyzed the data; N.S., M.H., and N.Y. controlled the data; S.W. wrote the paper; and all authors checked the final version of the manuscript.

Conflict-of-interest statement: The authors declare no competing financial interests.

Correspondence: Naoki Yamamoto, AIDS Research Center, National Institute of Infectious Diseases, 1-23-1 Toyama, Shinjuku-ku, Tokyo 162-8640, Japan; e-mail: nyama@nih.go.jp; Mitsuo Honda, AIDS Research Center, National Institute of Infectious Diseases, 1-23-1 Toyama, Shinjuku-ku, Tokyo 162-8640, Japan; e-mail: mhonda@nih.go.jp; and Norio Shimizu, Department of Virology, Division of Medical Science, Medical Research Institute, Tokyo Medical and Dental University, 1-5-45 Yushima, Bunkyo-ku, Tokyo 113-8519, Japan; e-mail: nshivir@umd.ac.jp.

References

1. Letvin NL, Barouch DH, Montefiori DC. Prospects for vaccine protection against HIV-1 infection and AIDS. Annu Rev Immunol. 2002;20:73-99.
2. Namikawa R, Kaneshima H, Lieberman M, Weissman IL, McCune JM. Infection of the SCID-hu mouse by HIV-1. Science. 1988;242: 1684-1686.
3. Bonyhadi ML, Rabin L, Salimi S, et al. HIV induces thymus depletion in vivo. Nature. 1993; 363:728-732.
4. Aldrovandi GM, Feuer G, Gao L, et al. The SCID-hu mouse as a model for HIV-1 infection. Nature. 1993;363:732-736.
5. Su L, Kaneshima H, Bonyhadi M, et al. HIV-1-induced thymocyte depletion is associated with indirect cytopathogenicity and infection of progenitor cells in vivo. Immunity. 1995;2:25-36.
6. Kaneshima H, Su L, Bonyhadi ML, Connor RI, Ho DD, McCune JM. Rapid-high, syncytium-inducing isolates of human immunodeficiency virus type 1 induce cytopathicity in the human thymus of the SCID-hu mouse. J Virol. 1994;68:8188-8192.
7. Jenkins M, Hanley MB, Moreno MB, Wieder E, McCune JM. Human immunodeficiency virus-1 infection interrupts thymopoiesis and multilineage hematopoiesis in vivo. Blood. 1998;91:2672-2678.
8. Koka PS, Fraser JK, Bryson Y, et al. Human immunodeficiency virus inhibits multilineage hematopoiesis in vivo. J Virol. 1998;72:5121-5127.
9. Mosier DE, Gulizia RJ, Baird SM, Wilson DB, Spector DH, Spector SA. Human immunodeficiency virus infection of human-PBL-SCID mice. Science. 1991;251:791-794.
10. Torbett BE, Picchio G, Mosier DE. hu-PBL-SCID mice: a model for human immune function, AIDS, and lymphomagenesis. Immunol Rev. 1991;124: 139-164.
11. Ruxrungtham K, Boone E, Ford H Jr, Driscoll JS, Davey RT Jr, Lane HC. Potent activity of 2'-beta-fluoro-2',3'-dideoxyadenosine against human immunodeficiency virus type 1 infection in hu-PBL-SCID mice. Antimicrob Agents Chemother. 1996;40:2369-2374.
12. Mosier DE, Gulizia RJ, MacIsaac PD, Torbett BE, Levy JA. Rapid loss of CD4+ T cells in human-PBL-SCID mice by noncytopathic HIV isolates. Science. 1993;260:689-692.
13. Koyanagi Y, Tanaka Y, Kira J, et al. Primary human immunodeficiency virus type 1 viremia and central nervous system invasion in a novel hu-PBL-immunodeficient mouse strain. J Virol. 1997; 71:2417-2424.
14. Tary-Lehmann M, Saxon A, Lehmann PV. The human immune system in hu-PBL-SCID mice. Immunol Today. 1995;16:529-533.
15. Ito M, Hiramatsu H, Kobayashi K, et al. NOD/SCID/gamma(c)(null) mouse: an excellent recipient mouse model for engraftment of human cells. Blood. 2002;100:3175-3182.
16. Yahata T, Ando K, Nakamura Y, et al. Functional human T lymphocyte development from cord blood CD34+ cells in nonobese diabetic/Shi-scid, IL-2 receptor gamma null mice. J Immunol. 2002; 169:204-209.
17. Hiramatsu H, Nishikomori R, Heike T, et al. Complete reconstitution of human lymphocytes from cord blood CD34+ cells using the NOD/SCID/gammacnull mice model. Blood. 2003;102:873-880.
18. Matsumura T, Kametani Y, Ando K, et al. Functional CD5+ B cells develop predominantly in the spleen of NOD/SCID/gammac(null) (NOG) mice transplanted either with human umbilical cord blood, bone marrow, or mobilized peripheral blood CD34+ cells. Exp Hematol. 2003;31:789-797.
19. Shinohara K, Sakai K, Ando S, et al. A highly pathogenic simian/human immunodeficiency virus with genetic changes in cynomolgus monkey. J Gen Virol. 1999;80:1231-1240.
20. Yamakami K, Honda M, Takei M, et al. Early bone marrow hematopoietic defect in simian/human immunodeficiency virus C2/1-infected macaques and relevance to advance of disease. J Virol. 2004;78:10906-10910.
21. Nakata H, Maeda K, Miyakawa T, et al. Potent anti-R5 human immunodeficiency virus type 1 effects of a CCR5 antagonist, AK602/ONO4128/GW873140, in a novel human peripheral blood mononuclear cell nonobese diabetic-SCID, interleukin-2 receptor gamma-chain-knocked-out AIDS mouse model. J Virol. 2005;79:2087-2096.
22. Heath SL, Tew JG, Tew JG, Szakal AK, Burton GF. Follicular dendritic cells and human immunodeficiency virus infectivity. Nature. 1995;377:740-744.
23. Orenstein JM, Fox C, Wahl SM. Macrophages as a source of HIV during opportunistic infections. Science. 1997;276:1857-1861.
24. van Kooyk Y, Geijtenbeek TB. A novel adhesion pathway that regulates dendritic cell trafficking and T cell interactions. Immunol Rev. 2002;186: 47-56.
25. Taylor JR Jr, Kimbrell KC, Scoggins R, Delaney M, Wu L, Camerini D. Expression and function of chemokine receptors on human thymocytes: implications for infection by human immunodeficiency virus type 1. J Virol. 2001;75:8752-8760.
26. Bleul CC, Wu L, Hoxie JA, Springer TA, Mackay CR. The HIV coreceptors CXCR4 and CCR5 are differentially expressed and regulated on human T lymphocytes. Proc Natl Acad Sci U S A. 1997; 94:1925-1930.
27. Fais S, Lapenta C, Santini SM, et al. Human immunodeficiency virus type 1 strains R5 and X4 induce different pathogenic effects in hu-PBL-SCID mice, depending on the state of activation/differentiation of human target cells at the time of primary infection. J Virol. 1999;73:6453-6459.
28. Gartner S, Markovits P, Markovitz DM, Kaplan MH, Gallo RC, Popovic M. The role of mononuclear phagocytes in HTLV-III/LAV infection. Science. 1986;233:215-219.
29. Koyanagi Y, Miles S, Mitsuyasu RT, Merrill JE, Vinters HV, Chen IS. Dual infection of the central nervous system by AIDS viruses with distinct cellular tropisms. Science. 1987;236:819-822.
30. Gendelman HE, Orenstein JM, Baca LM, et al. The macrophage in the persistence and pathogenesis of HIV infection. AIDS. 1989;3:475-495.
31. Embretson J, Zupancic M, Ribas JL, et al. Massive covert infection of helper T lymphocytes and macrophages by HIV during the incubation period of AIDS. Nature. 1993;362:359-362.
32. Igarashi T, Brown CR, Endo Y, et al. Macrophage are the principal reservoir and sustain high virus loads in rhesus macaques after the depletion of CD4+ T cells by a highly pathogenic simian immunodeficiency virus/HIV type 1 chimera (SHIV): implications for HIV-1 infections of humans. Proc Natl Acad Sci U S A. 2001;98:658-663.
33. Mir N, Costelio C, Luckit J, Lindley R. HIV-disease and bone marrow changes: a study of 60 cases. Eur J Haematol. 1989;42:339-343.
34. Moses A, Nelson J, Bagby GC Jr. The influence of human immunodeficiency virus-1 on hematopoiesis. Blood. 1998;91:1479-1495.
35. Koka PS, Jamieson BD, Brooks DG, Zack JA. Human immunodeficiency virus type 1-induced hematopoietic inhibition is independent of productive infection of progenitor cells in vivo. J Virol. 1999;73:9089-9097.
36. Koka PS, Kitchen CM, Reddy ST. Targeting c-Mpl for revival of human immunodeficiency virus type 1-induced hematopoietic inhibition when CD34+ progenitor cells are re-engrafted into a fresh stromal microenvironment in vivo. J Virol. 2004;78: 11385-11392.
37. Hillyer CD, Lackey DA 3rd, Villinger F, Winton EF, McClure HM, Ansari AA. CD34+ and CFU-GM progenitors are significantly decreased in SIVsmm9 infected rhesus macaques with minimal evidence of direct viral infection by polymerase chain reaction. Am J Hematol. 1993;43:274-278.
38. Thiebot H, Louache F, Vaslin B, et al. Early and persistent bone marrow hematopoiesis defect in simian/human immunodeficiency virus-infected macaques despite efficient reduction of viremia by highly active antiretroviral therapy during primary infection. J Virol. 2001;75:11594-11602.
39. Thiebot H, Vaslin B, Derdouch S, et al. Impact of bone marrow hematopoiesis failure on T-cell generation during pathogenic simian immunodeficiency virus infection in macaques. Blood. 2005; 105:2403-2409.

JOURNAL OF CLINICAL MICROBIOLOGY, Feb. 2007, p. 477–487
0095-1137/07/$08.00+0 doi:10.1128/JCM.01708-06

Vol. 45, No. 2

Use of New T-Cell-Based Cell Lines Expressing Two Luciferase Reporters for Accurately Evaluating Susceptibility to Anti-Human Immunodeficiency Virus Type 1 Drugs▽

Tomoko Chiba-Mizutani,[1,2] Hideka Miura,[1] Masakazu Matsuda,[1] Zene Matsuda,[1] Yoshiyuki Yokomaku,[1] Kosuke Miyauchi,[1] Masako Nishizawa,[1] Naoki Yamamoto,[1,2] and Wataru Sugiura[1]*

AIDS Research Center, National Institute of Infectious Diseases, Tokyo, Japan,[1] and Department of Molecular Virology and Microbiology, Tokyo Medical and Dental University, Tokyo, Japan[2]

Received 17 August 2006/Returned for modification 25 October 2006/Accepted 11 December 2006

Two new T-cell-based reporter cell lines were established to measure human immunodeficiency virus type 1 (HIV-1) infectivity. One cell line naturally expresses CD4 and CXCR4, making it susceptible to X4-tropic viruses, and the other cell line, in which a CCR5 expression vector was introduced, is susceptible to both X4- and R5-tropic viruses. Reporter cells were constructed by transfecting the human T-cell line HPB-Ma, which demonstrates high susceptibility to HIV-1, with genomes expressing two different luciferase reporters, HIV-1 long terminal repeat-driven firefly luciferase and cytomegalovirus promoter-driven renilla luciferase. Upon HIV infection, the cells expressed firefly luciferase at levels that were highly correlated (r^2 = 0.91 to 0.98) with the production of the capsid antigen p24. The cells also constitutively expressed renilla luciferase, which was used to monitor cell numbers and viability. The reliability of the cell lines for two in vitro applications, drug resistance phenotyping and drug screening, was confirmed. As HIV-1 efficiently replicated in these cells, they could be used for multiple-round replication assays as an alternative method to a single-cycle replication protocol. Coefficients of variation for drug susceptibility evaluated with the cell lines ranged from 17 to 41%. The new cell lines were beneficial for evaluating antiretroviral drug resistance. Firefly luciferase gave a wider dynamic range for evaluating virus infectivity, and the introduction of renilla luciferase improved assay reproducibility. The cell lines were also beneficial for screening new antiretroviral agents, as false inhibition caused by the cytotoxicity of test compounds was easily detected by monitoring renilla luciferase activity.

Drug resistance assays have been accepted as standard clinical tests to guide the antiretroviral therapy of human immunodeficiency virus (HIV)-infected patients who have developed resistance to drug treatment or drug-naïve patients infected with drug-resistant virus. These tests have been shown to improve treatment outcomes by selecting the most effective drugs and by minimizing the risk of treatment failure (2, 5–7, 9, 34). Drug resistance has been determined by two approaches. One is drug resistance genotyping, in which drug resistance is evaluated by sequencing the viral genes targeted by the drug, such as the HIV-1 protease and reverse transcriptase (RT) genes. The level of drug resistance is estimated by using observed mutation patterns and interpretation algorithms (23). Several protocols have been used for drug resistance genotyping, including in-house sequencing (10, 13, 38). Although these protocols differ in some aspects, e.g., the design of primers, the length of analyses, and amplification procedures, all are based on the same technical approach, modified Sanger sequencing.

The other approach to drug resistance assays is phenotyping. In this method, the levels of drug resistance of patient-derived viral isolates are evaluated by using in vitro bioassays (17, 26). Two advantages of the phenotyping assay are its ability to directly evaluate the drug susceptibilities of patient-derived viruses and the ease of interpreting its results compared to those from genotyping. This assay is especially useful in cases with a high degree of exposure to antiretroviral drugs, therefore involving many mutations. In these cases, the evaluation of resistance levels by genotyping alone may be difficult (35). In addition, the resistance levels determined by phenotyping provide important information for updating interpretation algorithms used in genotyping.

Although peripheral blood mononuclear cells (PBMC) are the natural target of HIV type 1 (HIV-1) and hence are the best candidates for host cells in phenotyping assays, reporter cell systems are more commonly used in drug susceptibility assays (1, 12, 15, 31). Reporter systems are preferred because their susceptibility to HIV-1 is stable and their output is both rapidly measured and highly reproducible compared to that of PBMC assays. Several kinds of reporter cells have been used with different reporter proteins, such as MAGI cells with β-galactosidase (21), GHOST cells with enhanced green fluorescent protein (36), MOCHA cells with secreted alkaline phosphatase (24), and CEM.NKR-CCR5-Luc cells with luciferase (31). Although these systems use different cell lines, their basic strategies for evaluating HIV infectivity are similar (21, 36). The cell lines carry a reporter protein gene regulated by the HIV-1 long terminal repeat (LTR) promoter, inducing them to

* Corresponding author. Mailing address: AIDS Research Center, National Institute of Infectious Diseases, 4-7-1 Gakuenn, Musashimurayama, Tokyo 2080011, Japan. Phone: 81-42-561-0771. Fax: 81-42-561-7746. E-mail: wsugiura@nih.go.jp.

▽ Published ahead of print on 20 December 2006.

produce the reporter protein when they are infected with HIV-1. Which reporter system is used depends on the properties of the original cell line and the installed reporter protein.

Reporter systems using MAGI and GHOST cells have the advantages of high sensitivity and rapidity in determining infectivity. However, MAGI and GHOST cells have been established from HeLa cells (21) and human osteosarcoma cells (36), respectively, which are not naturally susceptible to HIV-1. Therefore, these cells cannot propagate viruses efficiently. On the other hand, MOCHA and CEM.NKR-CCR5-Luc cell lines were established from T-cell lines and secreted alkaline phosphatase and luciferase, respectively, were installed as reporters. These reporter systems allow for the evaluation of HIV-1 infectivity by using enzymatic reactions and demonstrate greater reproducibility with wider dynamic ranges of reporter proteins. However, for these cells to produce sufficient reporter protein for accurate determinations, they must be cultured for 5 to 7 days, longer than MAGI and GHOST cells. Longer culture periods allow reporter cells to divide, which may affect the accuracy of the quantification.

Given the advantages and limitations of previously constructed reporter cell lines, we designed and tested two new reporter cell lines with dual chemokine receptors for use in drug resistance phenotypic assays and other HIV infectivity assays. The cell lines we designed have unique characteristics in that they originate from the human T-cell line HPB-Ma (16, 29, 40) and were engineered to express the CCR5 receptor and two different marker proteins, firefly luciferase (FL) and renilla luciferase (RL). FL, which is under HIV-1 LTR promoter regulation, is produced upon HIV-1 infection. Therefore, firefly luciferase activity can be used as a marker for virus infectivity. RL, which is under cytomegalovirus (CMV) promoter control, is constitutively expressed in the cells. Therefore, renilla luciferase activity can be used as a marker for cell number and viability.

MATERIALS AND METHODS

Construction of luciferase and CCR5 expression vectors. Two different luciferase expression vectors were constructed. The first luciferase construct comprised HIV-1 Tat-regulated FL and the red fluorescent protein (DsRed) construct 53LTRN-lucneo^r#1. The HIV-1 Tat-responsive reporter construct 53LTRN-lucneo^r#1 was constructed based on the expression vector pGEM-7Zf(+) (Promega, Madison, WI). Initially, a parent vector was constructed, 53LTRNCNS, which has a rabbit β-globin unit under the control of the HIV-1 LTR derived from strain HXB2. In this construct, a gene of interest can be cloned within the second exon of the β-globin gene and the polyadenylation signal is provided by the β-globin unit. A neomycin expression module was prepared by PCR and cloned upstream of the HIV-1 LTR region to generate 53LTRCNSneo. The reporter gene employed here was a fusion between an FL gene and a DsRed gene. The FL gene allows HIV-1 replication to be quantitatively evaluated by using luciferase activity when the LTR is activated by HIV-derived Tat, and the DsRed gene allows transfected and HIV-infected cells to be identified by red fluorescence. The FL portion was derived from pGLuc5 (Promega), and the DsRed portion was derived from pDsRed1N-1 (Clontech). Both genes were prepared by PCR, fused, and cloned into the β-globin unit by using NcoI and NotI restriction sites.

The second luciferase construct, pRenillaPac, was constructed using the plasmid pPUR (Clontech). The PCR-amplified RL gene, derived from phRL-CMV (Promega), was spliced into the upstream region of the *pac* gene. This hybrid gene manifests both RL activity and resistance to puromycin. Expression of the fusion gene was constitutive under the control of a CMV promoter.

A CCR5 expression vector, pCCR5/CEP4, was constructed based on the pCEP4 expression vector (Invitrogen), which possesses the Epstein-Barr nuclear antigen 1 episomal-expression gene. The CCR5 gene was inserted into the vector by using NotI and SnaB I restriction sites on the vector. Expression of the CCR5 gene was constitutive under the control of a CMV promoter.

Selection of host cell line and establishment of new reporter cell lines. To design new reporter cell lines for quantifying HIV-1 replication, we selected the murine leukemia virus-transformed human T-cell line HPB-Ma, established by Y. K. Shimizu and H. Yoshikura (16, 29, 40), because of its high susceptibility to HIV-1 and its stable expression of CD4 and CXCR4. HPB-Ma cells were maintained at 37°C in 5% CO_2 in complete RPMI 1640 medium (Sigma, Tokyo, Japan) supplemented with 10% fetal calf serum (HyClone, Logan, UT) and 1% penicillin-streptomycin (Invitrogen, Tokyo, Japan). Cells were transfected by electroporation with the two luciferase expression vectors, 53LTRN-lucneo^r#1 and pRenillaPac. Plasmid DNA (10 μg) was mixed with HPB-Ma cells (5×10^6 cells in 500 μl phosphate-buffered saline), and the mixture was incubated for 5 min at 4°C and electropulsed with a Gene Pulser II apparatus (Bio-Rad, Hercules, CA) at 250 V and 950 μF. After electroporation, the cells were resuspended in complete medium and incubated at 37°C in 5% CO_2. Subsequently, cells with incorporated plasmids were selected with 0.1 μg/ml puromycin (BD Biosciences, San Jose, CA) and 250 μg/ml Geneticin (Invitrogen), maintained in complete medium for several weeks, and enriched with cell populations expressing high levels of CD4 and CXCR4 by fluorescence-activated cell sorting with a FACSVantage system (BD Biosciences). Finally, clones were generated by limiting dilution and selected if they showed high sensitivity to HIV-1 and low spontaneous expression of FL and DsRed.

Since the parent HPB-Ma cell line expresses only the CXCR4 receptor, we extended the spectrum of the reporter cell lines to include R5-tropic viral isolates by transfecting cells by electroporation with a CCR5 expression plasmid. Clones were selected by incubating for several weeks with 0.1 μg/ml puromycin, 250 μg/ml Geneticin, and 150 μg/ml hygromycin B. Selected cells were recloned, and the expression of cell surface markers was confirmed by using FACSCaliber (Becton Dickinson, San Jose, CA). CD4, CXCR4, and CCR5 receptors were stained with SK-3-Cy5.5, 12G5-phycoerythrin, and 2D7-fluorescein isothiocyanate monoclonal antibodies, respectively (all from BD Biosciences, San Jose, CA).

Evaluation of introduced reporter gene functions. To confirm the ability of FL activity to reliably measure virus titer and production, established cell lines were plated into 96-well plates at 10^5 cells per well and inoculated with 50 to 400 50% tissue culture infective doses ($TCID_{50}$) of HXB2 or JRCSF. After 7 days of culture with the test viruses, cells were harvested and lysed in 75 μl of luciferase assay reagent. FL activity was quantified using a Dual-Glo luciferase reporter assay system (Promega, Madison, WI) and an LMax microplate luminometer (Molecular Devices, Sunnyvale, CA). Virus production was also quantified by using the p24 antigen enzyme-linked immunosorbent assay RETROtek kit (ZeproMetrix Co., Buffalo, NY) and compared with FL activity.

The validity of using RL activity to monitor MaRBLE cell numbers was evaluated by measuring RL activity in various numbers of cells and determining the correlation between RL activity and cell numbers. The correlation between RL activity and cell viability was also confirmed in cell killing assays with two anticancer drugs, hygromycin B (Invitrogen, Tokyo, Japan) and blasticidin S (Funakoshi, Tokyo, Japan). Target cells were plated into 96-well plates at 10^5 cells per well, and hygromycin B (15.6 to 500 μg/ml) and blasticidin S (1.25 to 20 μg/ml) were added. After 7 days of culture, cells were harvested and RL activity was measured by using the Dual-Glo luciferase reporter assay system (Promega) and the percentage of cell killing was determined by trypan blue staining.

Preparation of recombinant and patient-derived viruses. Recombinant viruses with point mutations were constructed as described elsewhere (25). In brief, drug resistance mutations were introduced into the RT and protease genes of the HXB2 clone by site-directed mutagenesis (28). MT-2 cells (5×10^6 human T-lymphoblastoid cells) were then transfected by electroporation with the recombinant virus plasmids, and the cells were maintained in 10 ml of complete medium for 7 to 14 days. Half the culture supernatant was harvested and replaced with fresh medium every other day. Viral replication was monitored by measuring RT activity in the supernatant, and the sample with the highest RT activity was used in subsequent studies.

Eight clinical samples were selected randomly from patient blood specimens sent for routine HIV-1 drug resistance testing to the AIDS Research Center, National Institute of Infectious Diseases, Tokyo, Japan. Patient viruses were isolated by a standard coculture method described elsewhere (18). In brief, 2×10^7 patient PBMC were mixed with the same number of phytohemagglutinin-stimulated normal human PBMC and the mixture was cultured for 2 weeks. Half the culture supernatant was collected and replaced with the same amount of fresh culture medium every other day. Viral replication was monitored by mea-

suring RT activity in the supernatant, and the sample with peak RT activity was selected and used for infection experiments afterward. RT assays were performed as previously described (37). Viral RNAs in collected supernatants were sequenced, and drug resistance mutation patterns were determined.

For the reconstructed virus, viral RNA was extracted from 200 μl of patient plasma by using a High Pure viral RNA kit (Roche, Basel, Switzerland) according to the manufacturer's instructions. Subsequently, a 1.8-kb *gag-pol* fragment, encoding the region from $p2^{gag}$ to whole protease, and the 5′ half of the RT gene fragment were amplified and inserted into the HXB2 backbone. MT-2 cells (5×10^6) were then transfected by electroporation with the plasmid, and the cells were maintained in 10 ml of complete medium for 7 to 14 days. Half the culture supernatant was harvested and replaced with fresh medium every other day. Viral replication was monitored by measuring RT activity in the supernatant, and the sample with the highest RT activity was selected for use in subsequent studies. Viral RNAs in collected supernatants were sequenced, and the drug resistance mutation patterns were confirmed. For both the patient-derived and reconstructed viruses, HIV infectivity ($TCID_{50}$) in the target cell lines was assayed by the Reed-Muench method (27).

Drug resistance genotyping. HIV-1 RNA was extracted from 200 μl of patient plasma using a High Pure viral RNA kit according to the manufacturer's instructions. For amplification of the 500-bp protease gene fragment, DRPRO5 (5′-AGA-CAG-GYT-AAT-TTT-TTA-GGG-A) and DRPRO2L (5′-TAT-GGA-TTT-TCA-GGC-CCA-ATT-TTT-GA) were used for reverse transcription and the first PCR and DRPRO1M (5′-AGA-GCC-AAC-AGC-CCC-ACC-AG) and DRPRO6 (5′-ACT-TTT-GGG-CCA-TCC-ATT-CC) were used for the second PCR. For amplification of the 800-bp RT gene fragment, DRRT1L (5′-ATG-ATA-GGG-GGA-ATT-GGA-GGT-TT) and DRRT4L (5′-TAC-TTC-TGT-TAG-TGC-TTT-GGT-TCC) were used for reverse transcription and the first PCR and DRRT7L (5′-GAC-CTA-CAC-CTG-TCA-ACA-TAA-TTG-G) and DRRT6L (5′-TAA-TCC-CTG-CAT-AAA-TCT-GAC-TTG-C) were used for the second PCR. The amplicons were purified by using a MultiScreen PCR filter plate (Millipore), and sequence reactions were performed by using the BigDye Terminator v3.1 cycle sequencing kit, followed by electrophoresis using an ABI-3730 auto sequencer (Applied Biosystems, Foster City, CA).

HIV-1 replication kinetics analyses and drug susceptibility assays. To analyze the replication kinetics of clinically derived HIV-1 isolates, target cells were plated into 96-well plates at 10^5 cells per well and infected with 100 $TCID_{50}$ of test viruses per well. At days 3, 5, and 7, the culture supernatant of each well was collected and RT activity was measured as previously described (37).

To evaluate anti-HIV-1 drug susceptibility, 10^7 cells were infected with 10,000 $TCID_{50}$ of wild-type control or test viruses in 50-ml tubes and incubated for 2 h at 37°C. Infected cells were resuspended in culture medium and plated into 96-well plates at 10^5 cells per well. At 2 and 48 h after infection, serial RT inhibitor dilutions and serial protease inhibitor (PI) dilutions were added, respectively. Each drug was prepared in a fivefold serial dilution and tested over different dose ranges, as follows. Didanosine, abacavir, and nevirapine were tested at concentrations from 25.0×10^1 μm to 3.2×10^{-4} μM. Lamivudine and stavudine were tested at concentrations from 5.0×10^1 μm to 6.4×10^{-5} μM. Zidovudine, zalcitabine, and the five PIs (saquinavir, indinavir, nelfinavir, lopinavir, and amprenavir) were tested at concentrations from 1.0×10^1 μm to 12.8×10^{-6} μM. Efavirenz was tested at concentrations from 0.2×10^1 μm to 25.6×10^{-7} μM. All samples were tested in triplicate. The following manufacturers kindly supplied anti-HIV drugs: GlaxoSmithKline, Middlesex, United Kingdom (zidovudine, lamivudine, and abacavir); Bristol-Myers Squibb, New York, NY (didanosine, stavudine, and efavirenz); Roche, Basel, Switzerland (zalcitabine and saquinavir); Boehringer Ingelheim, Ingelheim, Germany (nevirapine); Merck Research Laboratories, Rahway, NJ (indinavir); Japan Tobacco, Tokyo, Japan (nelfinavir); Vertex Pharmaceuticals, Cambridge, MA (amprenavir); and Abbott Laboratories, Abbott Park, IL (lopinavir).

After 7 days of culture with test drugs and test viruses, cells were harvested and lysed in 75 μl of luciferase assay reagent. Firefly and RL activities were sequentially quantified using a dual-luciferase reporter assay system (Promega) and an LMax microplate luminometer (Molecular Devices). Data were displayed by plotting the percentage of luciferase activity versus the $\log_{10}$ drug concentration. The concentration at which 50% of viral replication was inhibited (IC_{50}) was determined by plotting curves defined by the four-parametric sigmoidal equation $f(x) = A + ([B - A])/(1 + [C/x]^D)$ using XLfit4 software (CTC Laboratory Systems Corporation, Tokyo, Japan). To determine susceptibility or resistance, results for test viruses were compared to those for wild-type HIV-1 and evaluated by Student's *t* test.

RESULTS

Establishment of new T-cell-based cell lines with two luciferase reporter proteins. Two luciferase expression vectors were successfully constructed and used for transfection of the HPB-Ma cell line. These vectors were 53LTRN-lucneo^r#1, with FL under HIV-1 LTR regulation, and pRenillaPac, with RL under CMV promoter regulation. HPB-Ma cells with these vectors were subjected to several rounds of selection for cells resistant to Geneticin and puromycin and were enriched by flow cytometry with populations expressing high levels of CD4 and CXCR4 to establish the new cell line HPB-Ma/LTR-FL/CMV-RL (X4-MaRBLE).

Since the parent HPB-Ma cell line expresses only CXCR4, the spectrum of the X4-MaRBLE cell line was extended to include R5-tropic viruses by transfection with a CCR5 expression plasmid, thus establishing the R5-MaRBLE cell line. Expression levels of CD4 were comparable among the parent HPB-Ma, X4-MaRBLE, and R5-MaRBLE cell lines (Fig. 1a to c), whereas the proportion of CXCR4-positive cell populations and CXCR4 expression levels were slightly higher in X4- and R5-MaRBLE cells than in the parent HPB-Ma cell line (Fig. 1d to f). This difference is due to the cell sorter's selecting for populations expressing high levels of CXCR4. As for CCR5 expression, HPB-Ma and X4-MaRBLE cells did not significantly express the receptor (Fig. 1g and h). On the other hand, more than 76% of the R5-MaRBLE cell population expressed CCR5 (Fig. 1i).

To confirm the susceptibility of cell lines to X4- and R5-tropic viruses, each cell line was inoculated with HXB2 (X4-tropic) and JRCSF (R5-tropic) viruses. X4-MaRBLE cells inoculated with HXB2 expressed FL activity in a dose-dependent manner but did not show any FL activity after inoculation with JRCSF (Fig. 2a). On the other hand, R5-MaRBLE cells were susceptible to both HXB2 and JRCSF, which induced FL activity in a dose-dependent manner (Fig. 2b). To validate the use of FL activity to evaluate viral production, FL levels were compared to amounts of the viral capsid antigen, p24, in both X4- and R5-MaRBLE cell lines, and the correlation between FL levels and the amounts of p24 was determined. As shown in Fig. 2c, FL activity in cell lysates and the amount of p24 antigen in the culture supernatant were positively and linearly correlated in X4-MaRBLE cells infected with HXB2 ($r^2 = 0.98$), in R5-MaRBLE cells infected with HXB2 ($r^2 = 0.91$), and in R5-MaRBLE cells infected with JRCSF ($r^2 = 0.94$). These results verify that FL activity expressed by both X4- and R5-MaRBLE cell lines accurately represents the levels of viral replication and production. These good correlations also indicate a small likelihood of interference between the two LTRs in infected cells, the one driving luciferase and the other contained in the infecting virus.

The second type of luciferase, RL, was inserted into MaRBLE cells to monitor and evaluate their number and viability. As shown in Fig. 3a, RL activity demonstrated a positive, linear correlation with cell number ($r^2 = 0.99$). Thus, RL activity can be used to assess cell number in culture. Another useful parameter evaluated by RL activity was the cytotoxicity of test compounds added to cultures. To confirm the relationship between RL activity and cell viability, cell killing assays were performed with two anticancer drugs, hygromycin

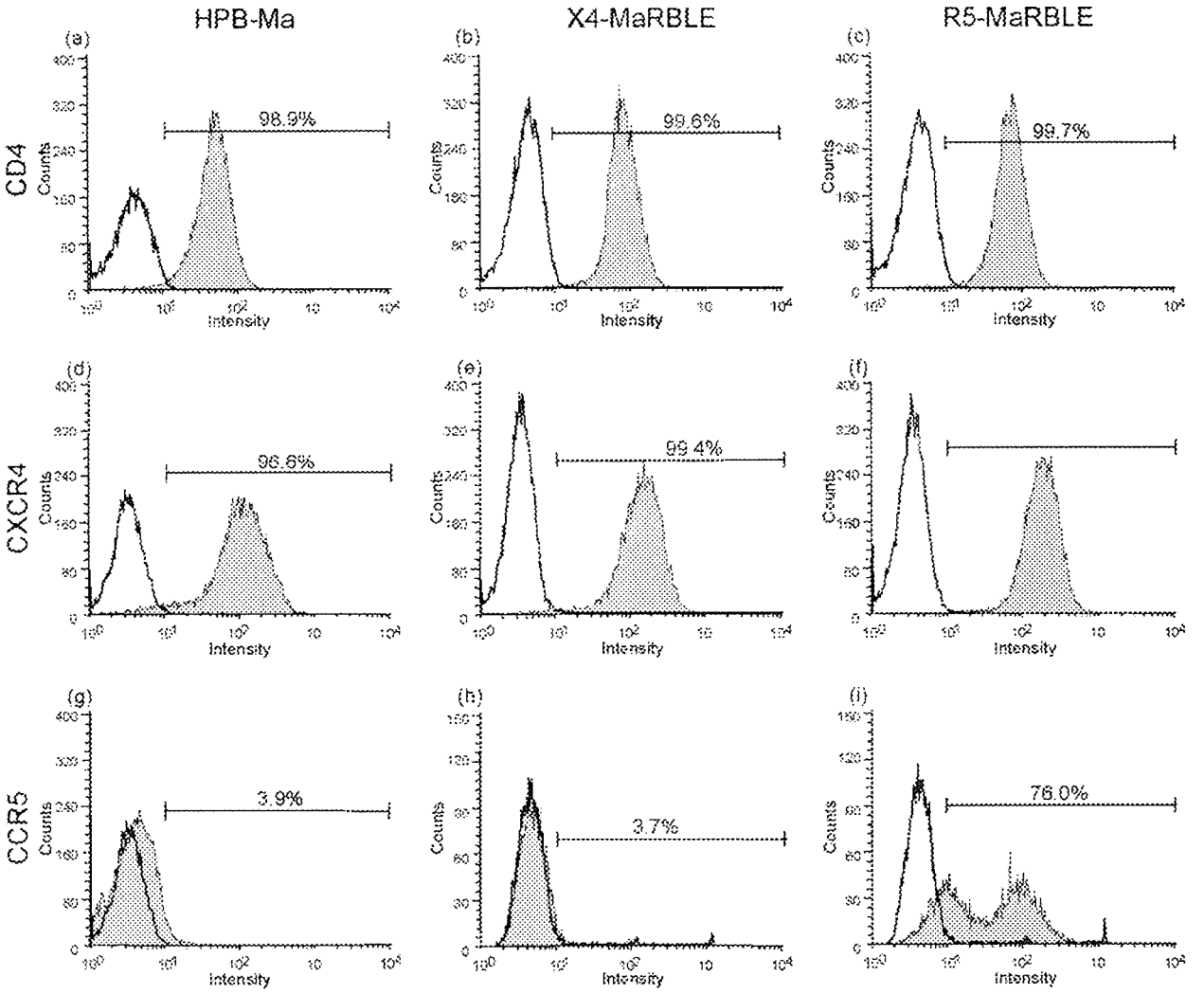

FIG. 1. Levels of expression of CD4, CXCR4, and CCR5 in parent HPB-Ma cells and X4-MaRBLE and R5-MaRBLE cells. Parent HPB-Ma (a, d, g), X4-MaRBLE (b, e, h), and R5-MaRBLE (c, f, i) cells were stained with monoclonal antibodies to CD4 (a, b, c), CXCR4 (d, e, f), and CCR5 (g, h, i). To calculate the percentage of each population positive for the expression of cytokine receptors (bars), 2,000 to 5,000 cells were analyzed by fluorescence-activated cell sorting. To calculate the percentage of each population positive for expression of CD4 and cytokine receptors (bar), 2,000 to 5,000 cells were analyzed by FACSCalibur and compared with fluorescence-negative control cells. Histograms with gray shading indicate cell populations stained with each monoclonal antibody; histograms without shading indicate negative control populations.

B (Fig. 3b) and blasticidin S (Fig. 3c). As the percentages of cells killed by both test chemicals increased, RL activity declined (Fig. 3b and c). The concentrations of hygromycin B and blasticidin S needed to kill 50% of the cells were 100 μg/ml and 2 μg/ml, respectively, in agreement with data from previous reports (3, 32). Thus, RL activity can be used to measure cytotoxicity.

In addition, the replication of two patient-derived viral isolates, 8 and 9, in R5-MaRBLE cells was compared to that in PBMC. As shown in Fig. 4, the two clinical isolates efficiently replicated in R5-MaRBLE cells. Isolate 8 replicated more efficiently in R5-MaRBLE cells than in PBMC, as indicated by the 10-fold-higher RT activity at day 7 in R5-MaRBLE cells (Fig. 4a). Isolate 9 had comparable day 7 RT activities in R5-MaRBLE cells and PBMC (Fig. 4b). These data clearly show that R5-MaRBLE cells can efficiently propagate clinical isolates.

Evaluation of HIV-1 drug susceptibility using X4- and R5-MaRBLE cells is highly reproducible. Having confirmed the quantitative reliability of FL expressed by HIV-infected X4- and R5-MaRBLE cell lines, we next used the cell lines to evaluate HIV-1 susceptibility to antiretroviral drugs. First, we evaluated the precision of phenotyping using the X4- and R5-MaRBLE cell lines. By using the wild-type HXB2 strain as a target virus for both X4- and R5-MaRBLE cells and JRCSF as a target virus for R5-MaRBLE cells, the IC_{50}s of four representative drugs from three classes of antiretroviral agents (zidovudine, lamivudine, efavirenz, and lopinavir) were determined by measuring FL activity. As shown in Fig. 5, well-characterized dose-response curves were obtained for the four drugs. The mean IC_{50}s, standard deviations (SD), and coefficients of variation (CV) for each cell line are summarized in Table 1. The CV ranged from 17 to 41%, demonstrating high reproducibility for drug susceptibility assays using both HIV-

FIG. 2. FL reporter activity in MaRBLE cells accurately represents viral production/chatn. (a) X4-MaRBLE cells are susceptible to HXB2 (X4-tropic) but not JRCSF (R5-tropic) viruses. FL activity was confirmed as a reliable measure of X4-tropic HIV-1 in X4-MaRBLE cells by inoculating the cells with various amounts of HXB2 or JRCSF and reading FL activity 7 days later. Solid and dashed lines indicate HXB2 and JRCSF, respectively. (b) R5-MaRBLE cells are susceptible to both HXB2 (X4-tropic) and JRCSF (R5-tropic) viruses. FL activity was confirmed as a reliable measure of X4- and R5-tropic HIV-1 in R5-MaRBLE cells by inoculating the cells with various amounts of HXB2 or JRCSF and reading FL activity 7 days later. Solid and dashed lines indicate HXB2 and JRCSF, respectively. (c) FL activity and the amount of capsid antigen p24 are correlated in HIV-infected MaRBLE cells. The reliability of using FL activity instead of the amount of p24 to quantify HIV-1 production was evaluated by measuring intracellular FL activity and the amount of p24 antigen in the supernatant from the same culture. Solid, dashed, and dotted lines indicate HXB2-infected X4-MaRBLE cells, HXB2-infected R5-MaRBLE cells, and JRCSF-infected R5-MaRBLE cells, respectively. Percentages of FL activity and of p24 production were calculated from the following formula: percentage = (observed value with the drug − background value)/(observed value without the drug − background value) × 100. RU, relative units.

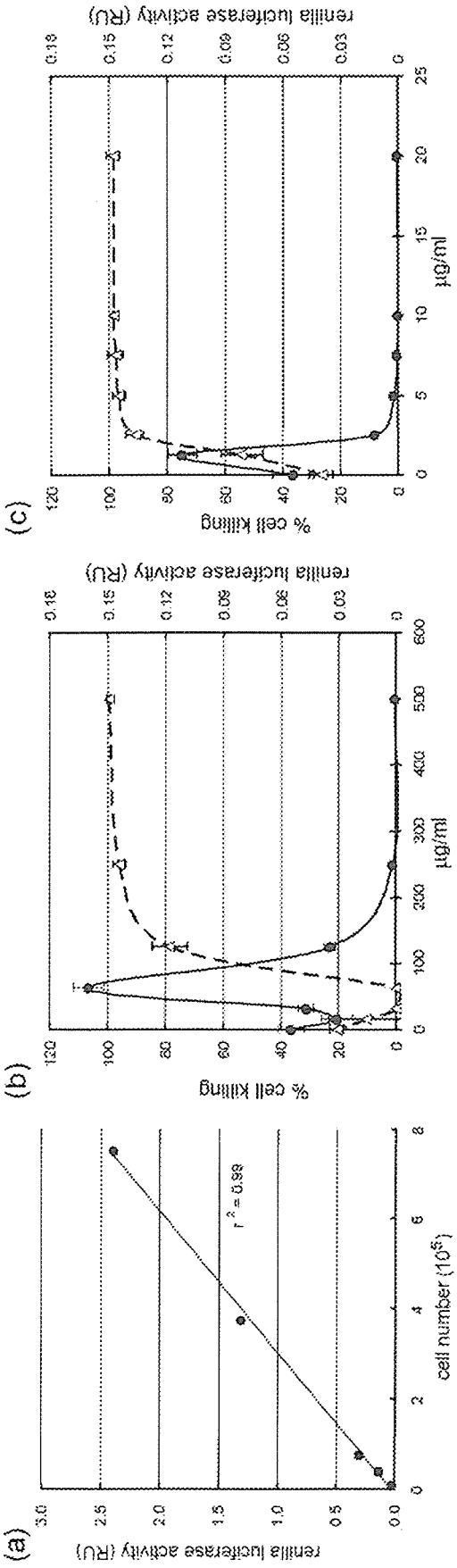

FIG. 3. Constitutively expressed RL in MaRBLE cells provides a reliable measure of cell number and viability. (a) RL activity accurately indicates MaRBLE cell numbers. The validity of using RL activity to monitor MaRBLE cell numbers was evaluated by measuring RL activity in various numbers of cells and plotting the corresponding values. RL activity and cell number were positively and linearly correlated ($r^2 = 0.99$). (b and c) RL activity reliably indicates hygromycin B and blasticidin S cytotoxicity in MaRBLE cells. The reliability of RL activity as a marker of cytotoxicity was evaluated for hygromycin B (b) and blasticidin S HCl (c). Cells were cultured for 1 week with serial dilutions of each drug and lysed, and their RL activities were determined. In graphs in both panels b and c, solid lines represent the RL activities of cell lysates and dashed lines indicate percentages of dead cells as determined by trypan blue staining. RU, relative units.

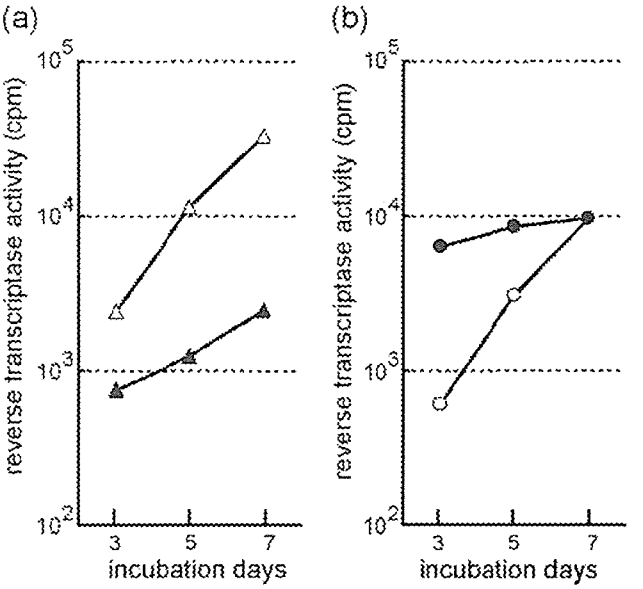

FIG. 4. Clinically derived isolates replicate in R5-MaRBLE cells as efficiently as in PBMC. The replication kinetics of two clinical isolates, 8 and 9, were compared after inoculation into both R5-MaRBLE cells and human PBMC. (a) Replication kinetics of isolate 8. Open and closed triangles indicate kinetics in R5-MaRBLE cells and PBMC, respectively. (b) Replication kinetics of isolate 9. Open and closed circles indicate kinetics in R5-MaRBLE cells and PBMC, respectively. cpm, counts per minute.

1-inoculated X4- and R5-MaRBLE cells. Interestingly, while the efavirenz and lopinavir susceptibilities of wild-type HXB2 were identical in evaluations with both X4- and R5-MaRBLE cells, the IC_{50}s for HXB2 and JRCSF were significantly different ($P < 0.001$) in the R5-MaRBLE cell line. Thus, in our assay, JRCSF appeared to be more susceptible than the HXB2 HIV-1 strain to efavirenz and slightly less resistant to lopinavir.

Drug susceptibility of drug-resistant HIV-1 can be evaluated using X4- and R5-MaRBLE cell lines. Given the accuracy and reproducibility of assays using MaRBLE cells to determine the drug susceptibilities of wild-type HXB2 and JRCSF, we then evaluated the reliability of using the cell lines for drug resistance phenotyping. Recombinant viruses with representative drug resistance mutations were constructed, and the drug resistance levels of the viruses were determined using X4-MaRBLE cells. The drug resistance levels associated with five patterns of nucleoside RT inhibitor (NRTI) resistance mutations are summarized in Table 2. Of the five mutant viral clones tested, four showed significant resistance to zidovudine, with resistance levels in the following order from lowest to highest: M41L/M184V/T215Y ≦ D67N/K70R < M41L/T215Y < M41L/D67N/K70R/T215Y. Thus, zidovudine resistance increased with the accumulation of thymidine analogue mutations (TAMs), and the M184V mutation caused reversion to the zidovudine resistance phenotype in the M41L/T215Y mutant, with a change in the susceptibility level of 12.5- to 3.5-fold relative to that of the wild-type virus, similar to results in previous reports (11, 19). Two clones with the M184V mutation demonstrated over 500-fold (>533.7- and >1,339.3-fold)-greater resistance to lamivudine but no significant resistance to didanosine and zalcitabine, although M184V has been re-

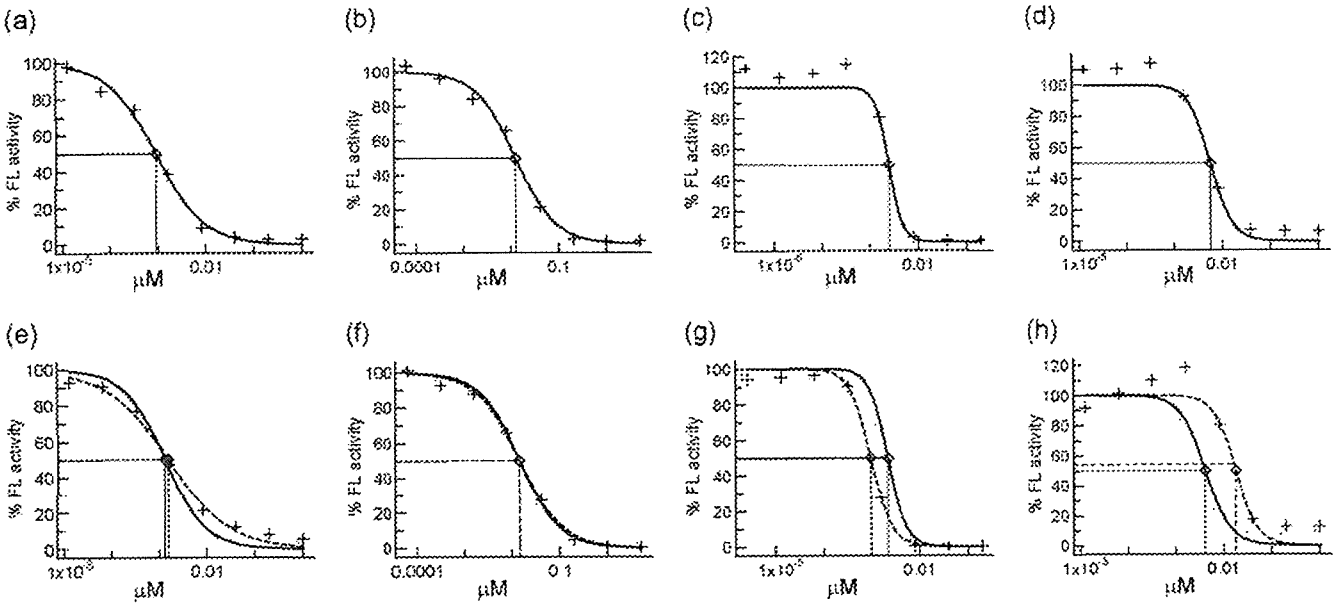

FIG. 5. Results of assays for HIV-1 drug susceptibility with MaRBLE reporter cell lines are highly reproducible. Dose-response curves for four representative agents against wild-type HXB2 and JRCSF are shown. Solid and dotted lines indicate HXB2 and JRCSF, respectively. (a to d) Results of assays for susceptibility to zidovudine, lamivudine, efavirenz, and lopinavir, respectively, using X4-MaRBLE cells. (e to h) Results of assays for susceptibility to zidovudine, lamivudine, efavirenz, and lopinavir, respectively, using R5-MaRBLE cells. The percentage of inhibition was calculated as follows: percentage = (observed FL activity with the drug − background FL activity)/(FL activity without the drug − background FL activity) × 100.

ported to confer a three- to fivefold increase in the level of resistance (14). Our data confirm the recent revalidation of using didanosine for cases involving the M184V mutation (39). Low-level but significant stavudine resistance in M41L/T215Y (change, 2.2-fold), M41L/M184V/T215Y (change, 2.9-fold), and M41L/D67N/K70R/T215Y (change, 3.8-fold) was found, consistent with data from previous reports (22, 33). All five clones demonstrated significant resistance to abacavir. The highest resistance was observed in the M41L/M184V/T215Y mutant, consistent with findings in previous reports that TAMs with M184V reduce susceptibility to abacavir 10-fold (1).

The drug resistance levels associated with the two most common nonnucleoside RT inhibitor (NNRTI) resistance mutations (K103N and Y181C) are summarized in Table 3. The K103N mutant virus demonstrated reduced susceptibility to both nevirapine (change, 78.6-fold) and efavirenz (change, 54.7-fold), whereas the Y181C virus was resistant only to nevirapine (change, 47.5-fold) but remained susceptible to efavirenz (change, 1.5-fold).

TABLE 1. Susceptibility of wild-type HXB2 and JRCSF to representative antiretrovirals as determined using X4- and R5-MaRBLE cells

Cell line	Agent	Mean IC_{50} (nM) ± SD (CV [%]) for[a]: HXB2 (n = 18)	HXB2 (n = 21)	JRCSF (n = 24)
X4-MaRBLE	Zidovudine	0.9 ± 0.4 (41)		
	Lamivudine	12.3 ± 3.9 (32)		
	Efavirenz	2.7 ± 1.0 (37)		
	Lopinavir	6.0 ± 1.0 (17)		
R5-MaRBLE	Zidovudine		1.3 ± 0.4 (31)	1.5 ± 0.6 (40)
	Lamivudine		13.6 ± 4.8 (35)	13.4 ± 3.6 (27)
	Efavirenz		2.1 ± 0.5[b] (24)	1.0 ± 0.3[b] (30)
	Lopinavir		4.2 ± 1.4[b] (33)	17.6 ± 6.9[b] (39)

[a] n, number of isolates of the indicated virus strain.
[b] IC_{50}s of efavirenz and lopinavir were significantly different for HXB2 and JRCSF in R5-MaRBLE cells ($P < 0.001$).

The drug resistance levels of three PI-resistant mutant clones (M46I, V82T, and L90M) are summarized in Table 4. Clones with M46I and L90M mutations did not demonstrate significant resistance to any PI tested, except for nelfinavir, to which the L90M clone demonstrated low-level (change, 3.3-fold) resistance. The clone with the V82T mutation demonstrated low-level resistance to indinavir (change, 3.8-fold), nelfinavir (change, 5.4-fold), amprenavir (change, 2.9-fold), and lopinavir (change, 5.0-fold), consistent with results in previous reports (8). Thus, the drug susceptibilities of viruses with resistance mutations evaluated with the MaRBLE cell lines matched those from previous reports of drug resistance, indicating the reliability of using the new cell lines to evaluate drug resistance.

To assess the reliability of using R5-MaRBLE cells to evaluate the levels of drug resistance of viral isolates from patients for whom treatment failed, seven cases were selected and viruses were isolated by coculture with normal human PBMC. Among the isolates from these seven cases, isolate 7 did not yield measurable virus by coculture. Therefore, a protease-RT gene fragment was amplified by RT-PCR and inserted into the HXB2 backbone. As shown in Table 5, isolate 1 had three minor mutations in the protease region and the virus was susceptible to all four inhibitors tested. The increase in resistance, calculated by comparison to the drug resistance of JRCSF, was <1.0-fold for zidovudine, lamivudine, and lopina-

TABLE 2. Drug resistance levels associated with NRTI resistance mutations as determined using X4-MaRBLE cells infected with HIV-1 clones

Agent	IC_{50} (nM) ± SD (change, *n*-fold)[a] for:					
	Wild type	M41L/T215Y	M184V	M41L/M184V/T215Y	D67N/K70R	M41L/D67N/K70R/T215Y
Zidovudine	0.8 ± 0.4	10.6 ± 6.9[c] (12.5 ± 1.9)	0.4 ± 0.1 (0.5 ± 0.01)	1.9 ± 1.0[b] (3.5 ± 0.5)	4.6 ± 1.0[c] (4.6 ± 1.2)	54.0 ± 32.3[c,d,e] (48.1 ± 16.0)
Didanosine	2,097.7 ± 1,101.4	2,899.8 ± 1,627.9 (1.4 ± 0.4)	2,164.6 ± 1,019.8 (1.3 ± 0.2)	2,893.7 ± 1519.0 (2.1 ± 0.8)	3,754.2 ± 1,468.3 (1.4 ± 0.3)	5,082.9 ± 2,397.5[b] (1.8 ± 0.5)
Zalcitabine	2.5 ± 1.1	3.8 ± 3.3 (1.5 ± 0.8)	3.4 ± 0.6 (1.3 ± 0.4)	3.9 ± 2.0 (2.2 ± 0.8)	3.0 ± 0.8 (1.2 ± 0.3)	3.5 ± 2.3 (1.2 ± 0.6)
Lamivudine	8.7 ± 4.5	20.9 ± 14.5[b] (3.8 ± 3.2)	>5,000[c] (>533.7)	>5,000[c] (>1,339.3)	17.8 ± 6.9[b] (2.4 ± 1.3)	44.3 ± 27.7[c] (6.8 ± 7.4)
Stavudine	14.4 ± 5.2	29.9 ± 14.0[b] (2.2 ± 0.4)	17.5 ± 7.6 (0.9 ± 0.3)	40.7 ± 23.8[b] (2.9 ± 1.1)	31.3 ± 24.9 (2.3 ± 1.7)	50.3 ± 24.2[c] (3.8 ± 1.6)
Abacavir	348.7 ± 122.8	985.5 ± 306.3[c] (3.2 ± 1.1)	1,497.5 ± 589.4[c] (3.9 ± 1.2)	3,300.0 ± 1,986.9[c,d] (10.6 ± 3.1)	836.2 ± 522.5[b] (2.1 ± 0.7)	2,015.1 ± 842.8[c,d] (5.2 ± 0.9)

[a] Change (*n*-fold) = (observed IC_{50} for strain)/(IC_{50} for wild type).
[b] P, <0.05 for comparison with wild-type virus.
[c] P, <0.005 for comparison with wild-type virus.
[d] P, <0.05 for comparison with M41L/T215Y virus.
[e] P, <0.05 for comparison with D67N/K70R virus.

vir. The patient in case 2 had been heavily treated with antiretroviral agents, and isolate 2 had a high accumulation of NRTI and PI resistance mutations but no NNRTI resistance mutation. This isolate had six TAMs and an M184V mutation in the RT region and demonstrated resistance to zidovudine (change, 32.9-fold) and lamivudine (change, >380.7-fold) but not to efavirenz. As for the protease region, 11 mutations were detected, including three major mutations (M46I, V82F, and L90M). Of these 11 mutations, 10 matched known lopinavir resistance mutations (International AIDS Society—USA drug resistance chart) (20). Indeed, high resistance to lopinavir (change, >76.5-fold) was observed.

Isolate 3 had 6 TAMs (M41L, E44D, D67N, V118I, L210W, and T215Y), and a high level of resistance to zidovudine (change, 114.5-fold) was observed. As the virus in this isolate had all four known NRTI resistance mutations responsible for hypersusceptibility to NNRTIs, it was hypersusceptible to efavirenz (change, 0.2-fold). Efavirenz hypersusceptibility was defined as a change in resistance of <0.4-fold compared to that of the wild type by statistical analysis (mean value minus 2 SD) and by data from a previous report (4). Isolate 4 had accumulated five TAMs and demonstrated 191.7-fold-higher resistance to zidovudine. No lamivudine resistance and NNRTI resistance mutations were observed, and the virus was susceptible to lamivudine. Isolate 4 also had M41L, V118I, L210W, and T215Y mutations, and the virus demonstrated hypersusceptibility to efavirenz (change, 0.2-fold). Two major mutations, D30N and L90M, and eight secondary mutations in the protease region were observed. Of these eight secondary mutations, five matched lopinavir resistance mutations, with our assay indicating a 9.4-fold increase in resistance to lopinavir. Isolate 5 had an RT inhibitor resistance pattern similar to that of isolate 2, having accumulated six TAMs and the M184V lamivudine resistance mutation in RT and demonstrating 104.1-fold-higher resistance to zidovudine and >380.7-fold-higher resistance to lamivudine. This virus also had M41L, V118I, L210W, and T215Y mutations. Though this virus appeared to be slightly more susceptible to efavirenz (change, 0.6-fold), this effect was not statistically significant. Isolate 5 had accumulated 11 lopinavir resistance mutations in the protease region and demonstrated 75.5-fold-higher resistance to lopinavir in our assay.

Isolate 6 had accumulated six TAMs in RT and showed 224.0-fold-higher resistance to zidovudine. This isolate had E44D and V118I mutations (low-level-lamivudine-resistance mutations) and showed 6.7-fold-higher resistance to lamivudine. Similar to those in cases 3 to 5, the virus in case 6 had M41L, V118I, L210W, and T215Y mutations and demonstrated slight hypersusceptibility to efavirenz (change, 0.4-fold). As for the protease region, isolate 6 had three major mutations, M46I, I84V, and L90M, and six minor resistance mutations. Of these nine mutations, eight were listed as lopinavir resistance mutations, and intermediate-level resistance to lopinavir (change, 14.6-fold) was observed. Isolate 7R had K103N and showed high-level resistance to efavirenz (change, 66.8-fold). No other drug resistance mutations in the RT region were found, and thus the isolate was susceptible to zidovudine and lamivudine. The protease region did show two minor mutations, L63C and V77I, and the isolate was susceptible to lopinavir.

TABLE 3. Drug resistance levels associated with NNRTI resistance mutations as determined using X4-MaRBLE cells infected with HIV-1 clones

Agent	IC_{50} (nM) ± SD (change, *n*-fold)[a] for:		
	Wild type	K103N	Y181C
Nevirapine	206.3 ± 68.2	16,110.7 ± 6,445.7[b] (78.6 ± 19.7)	9,586.3 ± 6,396.4[c] (47.5 ± 23.8)
Efavirenz	1.4 ± 0.4	79.3 ± 33.3[b] (54.7 ± 15.6)	2.3 ± 0.6[c] (1.5 ± 0.1)

[a] Change (*n*-fold) = (observed IC_{50} for strain)/(IC_{50} for wild type).
[b] P, <0.005 for comparison with wild-type virus.
[c] P, <0.05 for comparison with wild-type virus.

Thus, the increases observed in levels of resistance to zidovudine and lopinavir were associated with the accumulation of known resistance mutations associated with those drugs. Similarly, hypersusceptibility to efavirenz was associated with the accumulation of M41L, V118I, L210W, and T215Y mutations in four out of six clinical isolates (30). Taken together, these results confirm the reliability of using X4- and R5-MaRBLE cells in drug resistance phenotyping.

DISCUSSION

The development of reliable methodologies to evaluate drug susceptibility in vitro has been a major thrust of drug resistance research. Although several phenotypic assays are commercially available for clinical usage, they are expensive and may not be readily available either in developing or developed countries. As for use in research laboratories, these commercial assays target only the protease and reverse transcriptase gene regions of the HIV-1 genome, limiting their flexibility as a tool for basic research. Thus, there is still a need for easy-to-use assay systems with high reproducibility, for both clinical and research usage. To fill this gap, we drew a blueprint for a new type of reporter cell line by considering the advantages and drawbacks of several previously reported cell lines (12, 15, 17, 21, 24, 26, 31, 36). Based on this blueprint, we chose the T-cell-based cell line HPB-Ma (16, 29, 40) as the parent cell line to introduce reporter genes and to establish new reporter cell lines. HPB-Ma is a murine leukemia virus-transformed human T-cell line demonstrating high susceptibility to HIV-1, which can replicate efficiently in these host cells. As HPB-Ma cells naturally express CD4 and CXCR4, but not CCR5, we introduced the CCR5 expression gene to widen the susceptibility spectrum of the cell line to include R5-tropic viruses. The reporter protein chosen to measure HIV infectivity was FL, as it has a wider dynamic range than other known reporter candidates. Another type of luciferase, RL, was introduced as a marker of cell number and viability.

Finally, two types of new reporter cell lines were established, X4-MaRBLE and R5-MaRBLE. As expected, these new cell lines had several advantages over previously described cell lines. First, viruses efficiently propagated in these cell lines, making multiple-round replication assays possible. In addition, viruses could be isolated from patient plasma and PBMC by using the cell lines. Since other reporter cells may not allow replication-competent viruses to be efficiently produced, their use is largely limited to single-cycle replication assays. These assays are currently accepted as the major method for measuring viral infectivity due to their rapid readout of results. However, single-cycle replication assays cannot evaluate the postintegration late phase of the viral life cycle. To evaluate late-phase inhibitors, such as PIs, by using single-cycle replication assays, an additional step is required prior to the assay to produce viruses under test drug pressure. On the other hand, multiple-round replication assays allow late-phase inhibitors to be directly evaluated, just as early-phase inhibitors, without additional culture. Furthermore, multiple-round replication assays allow for a clearer readout of drug susceptibility, as the differences in drug susceptibilities between the reference and test viruses may be amplified by each round of replication.

Second, the cell lines were successfully transfected with RL to broaden their application. The constitutive expression of this second luciferase in the cell line has made it possible to easily and accurately evaluate cell number and the cytotoxicities of test compounds. As we planned to conduct multiple rounds of assays, the cells were cultured for at least a week, long enough for them to propagate and increase the background level of FL. The extent of this increase depended on the amount of viral inocula or the level of inhibition by antiretroviral agents. By monitoring RL activity,

TABLE 4. Drug resistance levels of PI-resistant mutants analyzed using HIV-1-infected X4-MaRBLE cells

Agent	IC_{50} (nM) ± SD (change, *n*-fold)[a] for:			
	Wild type	M46I	V82T	L90M
Indinavir	11.3 ± 4.3	19.5 ± 17.0 (2.2 ± 2.7)	38.0 ± 6.8[b] (3.8 ± 1.6)	11.5 ± 1.5 (1.1 ± 0.3)
Saquinavir	7.4 ± 3.4	5.0 ± 2.4 (0.7 ± 0.3)	6.5 ± 1.3 (1.0 ± 0.4)	6.9 ± 1.1 (1.0 ± 0.4)
Nelfinavir	4.9 ± 2.3	7.4 ± 5.3 (1.9 ± 1.5)	20.0 ± 5.5[b] (5.4 ± 3.7)	11.5 ± 0.7[d] (3.3 ± 2.2)
Amprenavir	6.7 ± 3.1	9.7 ± 5.4 (2.0 ± 2.0)	17.2 ± 5.2[c] (2.9 ± 1.0)	10.7 ± 2.1 (2.0 ± 1.3)
Lopinavir	6.6 ± 3.8	6.3 ± 2.9 (1.1 ± 0.7)	29.1 ± 9.0[c] (5.0 ± 1.8)	5.6 ± 0.9 (1.1 ± 0.7)

[a] Change (*n*-fold) = (observed IC_{50} for strain)/(IC_{50} for wild type).
[b] P, <0.005 for comparison with wild-type virus.
[c] P, <0.05 for comparison with wild-type virus.
[d] P, <0.01 for comparison with wild-type virus.

TABLE 5. Susceptibilities of seven patient-derived viral isolates to representative drugs assayed using R5-MaRBLE cells

Strain or isolate (subtype)	Tropism[b]	RT mutation(s)	Protease mutation(s)	IC_{50} (nM) ± SD (change, *n*-fold) of:			
				Zidovudine	Lamivudine	Efavirenz	Lopinavir
JRCSF (B)	R5	None	L63P	1.4 ± 0.6 (1)	13.6 ± 4.6 (1)	0.9 ± 0.1 (1)	19.3 ± 8.4 (1)
1 (B)	R5	None	L63P/T, A71A/V, V77I	1.2 (0.7)	4.2 (0.3)	1.5 (1.8)	6.8 (0.5)
2 (B)	X4, R5	M41L, D67N, K70R, K101Q, M184V, L210L/W, T215F, K219Q	L10I, L33F, M46I, F53L, I54V, L63P, A71V, G73S/T, V77I, V82F, L90M	56.1 (32.9)	>5,000 (>380.7)	1.1 (1.3)	>1,000 (>76.5)
3 (F)	X4, R5	M41L, E44E/D, D67N, K101K/E, V118I, L210W, T215Y	K20T, D30N, M36I, M46M/L, L63P, A71V, N88D	195.1 (114.5)	34.5 (2.6)	0.1 (0.2)	ND[c] (ND)
4 (B)	X4, R5	M41L, E44A, D67N, V118I, L210W, T215Y	L10V, K20T, D30N, M36I, I54V, L63T, A71V, V77V/I, N88D, L90M	326.5 (191.7)	13.5 (1.0)	0.2 (0.2)	123.4 (9.4)
5 (B)	X4, R5	M41L, E44D, D67N, V118I, M184V, L210W, T215Y	L10V, K20R, V32I, M36I, M46L, F53F/L, I54V, L63P, A71V, V82A, L90M	177.4 (104.1)	>5,000 (>380.7)	0.5 (0.6)	986.8 (75.5)
6 (F)	R5	M41L, E44D, D67N, V118I, L210W, T215Y	L10I, K20T, M36I, M46I, F53L, L63L/I/T/P, A71V, I84V, L90M	381.7 (224.0)	88.0 (6.7)	0.3 (0.4)	190.6 (14.6)
7R[a] (B)	X4	K103N	L63C, V77I	2.1 (1.5)	22.3 (1.6)	60.2 (66.8)	7.6 (0.4)

[a] Recombinant HXB2 with patient-derived protease and RT sequences.
[b] The tropism of each virus was determined by using X4-GHOST and R5-GHOST cells.
[c] ND, not determined.

we could easily evaluate culture conditions and their effects on assay results.

These two characteristics confer a great advantage to using the MaRBLE cell lines for screening new antiretroviral agents. They allow both early- and late-phase inhibitor candidates to be evaluated under the same protocol, as the assay permits multiple viral replications. Moreover, monitoring of RL activity allows false-positive results (inhibition by test drugs due to cytotoxicity) to be detected and eliminated. Finally, the use of RL activity greatly improved the efficacy of screening.

The MaRBLE cell lines stably expressed the transfected genes, as confirmed by the stable expression of CD4, CXCR4, and CCR5 on the surfaces of cells maintained in culture for up to 6 months with continuous passage. We also confirmed that the two reporter genes were stably expressed and that IC_{50}s were identical for both newly plated and 6-month-old cultures (data not shown).

In conclusion, we successfully established two unique cell lines, X4-MaRBLE and R5-MaRBLE, which are useful for assaying viral drug resistance and for screening new antiretroviral compounds. Although the cost of phenotypic assays using our cell lines may be less than that of commercial systems, the assays require a biosafety level 3 laboratory, general culture equipment, and a luminometer for readout. Since these are all expensive items, the assay price should be reduced and the assay protocol should be simplified for wider usage of the assay.

ACKNOWLEDGMENTS

We thank Hiroshi Yoshikura, Mari Takizawa, and Mitsuo Honda for their help and discussions. We also thank Claire Baldwin for her help in preparing the manuscript.

This study was supported by a grant from the Human Sciences Foundation and the Program for Promotion of Fundamental Studies in Health Sciences of the National Institute of Biomedical Innovation (NIBIO).

REFERENCES

1. **Ait-Khaled, M., A. Rakik, P. Griffin, A. Cutrell, M. A. Fischl, N. Clumeck, S. B. Greenberg, R. Rubio, B. S. Peters, F. Pulido, J. Gould, G. Pearce, W. Spreen, M. Tisdale, and S. Lafon.** 2002. Mutations in HIV-1 reverse transcriptase during therapy with abacavir, lamivudine and zidovudine in HIV-1-infected adults with no prior antiretroviral therapy. Antivir. Ther. **7**:43–51.
2. **Baxter, J. D., D. L. Mayers, D. N. Wentworth, J. D. Neaton, M. L. Hoover, M. A. Winters, S. B. Mannheimer, M. A. Thompson, D. I. Abrams, B. J. Brizz, J. P. Ioannidis, T. C. Merigan, et al.** 2000. A randomized study of antiretroviral management based on plasma genotypic antiretroviral resistance testing in patients failing therapy. AIDS **14**:F83–93.
3. **Bento, F. M., D. Takeshita, C. B. Sacramento, T. R. Machado, M. B. Mathor, A. K. Carmona, and S. W. Han.** 2004. Over expression of the selectable marker blasticidin S deaminase gene is toxic to human keratinocytes and murine BALB/MK cells. BMC Biotechnol. **4**:29.
4. **Bosch, R. J., G. F. Downey, D. A. Katzenstein, N. Hellmann, L. Bacheler, and M. A. Albrecht.** 2003. Evaluation of cutpoints for phenotypic hypersusceptibility to efavirenz. AIDS **17**:2395–2396.
5. **Cingolani, A., A. Antinori, M. G. Rizzo, R. Murri, A. Ammassari, F. Baldini, S. Di Giambenedetto, R. Cauda, and A. De Luca.** 2002. Usefulness of monitoring HIV drug resistance and adherence in individuals failing highly active antiretroviral therapy: a randomized study (ARGENTA). AIDS **16**:369–379.
6. **Clevenbergh, P., J. Durant, P. Halfon, P. del Giudice, V. Mondain, N. Montagne, J. M. Schapiro, C. A. Boucher, and P. Dellamonica.** 2000. Persisting long-term benefit of genotype-guided treatment for HIV-infected patients failing HAART. The Viradapt Study: week 48 follow-up. Antivir. Ther. **5**:65–70.
7. **Cohen, C. J., S. Hunt, M. Sension, C. Farthing, M. Conant, S. Jacobson, J. Nadler, W. Verbiest, K. Hertogs, M. Ames, A. R. Rinehart, and N. M. Graham.** 2002. A randomized trial assessing the impact of phenotypic resistance testing on antiretroviral therapy. AIDS **16**:579–588.
8. **Condra, J. H., W. A. Schleif, O. M. Blahy, L. J. Gabryelski, D. J. Graham, J. C. Quintero, A. Rhodes, H. L. Robbins, E. Roth, M. Shivaprakash, D. Titus, T. Yang, H. Teppler, K. E. Squires, P. J. Deutsch, and E. A. Emini.** 1995. In vivo emergence of HIV-1 variants resistant to multiple protease inhibitors. Nature **374**:569–571.
9. **Durant, J., P. Clevenbergh, P. Halfon, P. Delgiudice, S. Porsin, P. Simonet, N. Montagne, C. A. Boucher, J. M. Schapiro, and P. Dellamonica.** 1999. Drug-resistance genotyping in HIV-1 therapy: the VIRADAPT randomised controlled trial. Lancet **353**:2195–2199.
10. **Eshleman, S. H., G. Crutcher, O. Petrauskene, K. Kunstman, S. P. Cunningham, C. Trevino, C. Davis, J. Kennedy, J. Fairman, B. Foley, and J. Kop.** 2005. Sensitivity and specificity of the ViroSeq human immunodefi-

ciency virus type 1 (HIV-1) genotyping system for detection of HIV-1 drug resistance mutations by use of an ABI PRISM 3100 genetic analyzer. J. Clin. Microbiol. **43**:813–817.
11. **Fumero, E., and D. Podzamczer.** 2003. New patterns of HIV-1 resistance during HAART. Clin. Microbiol. Infect. **9**:1077–1084.
12. **Gervaix, A., D. West, L. M. Leoni, D. D. Richman, F. Wong-Staal, and J. Corbeil.** 1997. A new reporter cell line to monitor HIV infection and drug susceptibility in vitro. Proc. Natl. Acad. Sci. USA **94**:4653–4658.
13. **Grant, R. M., D. R. Kuritzkes, V. A. Johnson, J. W. Mellors, J. L. Sullivan, R. Swanstrom, R. T. D'Aquila, M. Van Gorder, M. Holodniy, R. M. Lloyd Jr., C. Reid, G. F. Morgan, and D. L. Winslow.** 2003. Accuracy of the TRUGENE HIV-1 genotyping kit. J. Clin. Microbiol. **41**:1586–1593.
14. **Gu, Z., Q. Gao, X. Li, M. A. Parniak, and M. A. Wainberg.** 1992. Novel mutation in the human immunodeficiency virus type 1 reverse transcriptase gene that encodes cross-resistance to 2′,3′- dideoxyinosine and 2′,3′-dideoxycytidine. J. Virol. **66**:7128–7135.
15. **Hachiya, A., S. Aizawa-Matsuoka, M. Tanaka, Y. Takahashi, S. Ida, H. Gatanaga, Y. Hirabayashi, A. Kojima, M. Tatsumi, and S. Oka.** 2001. Rapid and simple phenotypic assay for drug susceptibility of human immunodeficiency virus type 1 using CCR5-expressing HeLa/CD4(+) cell clone 1–10 (MAGIC-5). Antimicrob. Agents Chemother. **45**:495–501.
16. **Hartley, J. W., and W. P. Rowe.** 1976. Naturally occurring murine leukemia viruses in wild mice: characterization of a new "amphotropic" class. J. Virol. **19**:19–25.
17. **Hertogs, K., M. P. de Bethune, V. Miller, T. Ivens, P. Schel, A. Van Cauwenberge, C. Van Den Eynde, V. Van Gerwen, H. Azijn, M. Van Houtte, F. Peeters, S. Staszewski, M. Conant, S. Bloor, S. Kemp, B. Larder, and R. Pauwels.** 1998. A rapid method for simultaneous detection of phenotypic resistance to inhibitors of protease and reverse transcriptase in recombinant human immunodeficiency virus type 1 isolates from patients treated with antiretroviral drugs. Antimicrob. Agents Chemother. **42**:269–276.
18. **Hollinger, F. B., J. W. Bremer, L. E. Myers, J. W. Gold, L. McQuay, and the NIH/NIAID/DAIDS/ACTG Virology Laboratories.** 1992. Standardization of sensitive human immunodeficiency virus coculture procedures and establishment of a multicenter quality assurance program for the AIDS Clinical Trials Group. J. Clin. Microbiol. **30**:1787–1794.
19. **Imamichi, T.** 2004. Action of anti-HIV drugs and resistance: reverse transcriptase inhibitors and protease inhibitors. Curr. Pharm. Des. **10**:4039–4053.
20. **Johnson, V. A., F. Brun-Vezinet, B. Clotet, B. Conway, D. R. Kuritzkes, D. Pillay, J. M. Schapiro, A. Telenti, and D. D. Richman.** 2005. Update of the drug resistance mutations in HIV-1: fall 2005. Top. HIV Med. **13**:125–131.
21. **Kimpton, J., and M. Emerman.** 1992. Detection of replication-competent and pseudotyped human immunodeficiency virus with a sensitive cell line on the basis of activation of an integrated beta-galactosidase gene. J. Virol. **66**:2232–2239.
22. **Larder, B. A., S. D. Kemp, and P. R. Harrigan.** 1995. Potential mechanism for sustained antiretroviral efficacy of AZT-3TC combination therapy. Science **269**:696–699.
23. **Larder, B. A., A. Kohli, P. Kellam, S. D. Kemp, M. Kronick, and R. D. Henfrey.** 1993. Quantitative detection of HIV-1 drug resistance mutations by automated DNA sequencing. Nature **365**:671–673.
24. **Miyake, H., Y. Iizawa, and M. Baba.** 2003. Novel reporter T-cell line highly susceptible to both CCR5- and CXCR4-using human immunodeficiency virus type 1 and its application to drug susceptibility tests. J. Clin. Microbiol. **41**:2515–2521.
25. **Myint, L., M. Matsuda, Z. Matsuda, Y. Yokomaku, T. Chiba, A. Okano, K. Yamada, and W. Sugiura.** 2004. Gag non-cleavage site mutations contribute to full recovery of viral fitness in protease inhibitor-resistant human immunodeficiency virus type 1. Antimicrob. Agents Chemother. **48**:444–452.
26. **Petropoulos, C. J., N. T. Parkin, K. L. Limoli, Y. S. Lie, T. Wrin, W. Huang, H. Tian, D. Smith, G. A. Winslow, D. J. Capon, and J. M. Whitcomb.** 2000. A novel phenotypic drug susceptibility assay for human immunodeficiency virus type 1. Antimicrob. Agents Chemother. **44**:920–928.
27. **Reed, L., and H. Muench.** 1938. A simple method of estimating fifty percent endpoint. Am. J. Hyg. **27**:493–497.
28. **Sarkar, G., and S. S. Sommer.** 1990. The "megaprimer" method of site-directed mutagenesis. BioTechniques **8**:404–407.
29. **Shimizu, Y. K., R. H. Purcell, and H. Yoshikura.** 1993. Correlation between the infectivity of hepatitis C virus in vivo and its infectivity in vitro. Proc. Natl. Acad. Sci. USA **90**:6037–6041.
30. **Shulman, N. S., R. J. Bosch, J. W. Mellors, M. A. Albrecht, and D. A. Katzenstein.** 2004. Genetic correlates of efavirenz hypersusceptibility. AIDS **18**:1781–1785.
31. **Spenlehauer, C., C. A. Gordon, A. Trkola, and J. P. Moore.** 2001. A luciferase-reporter gene-expressing T-cell line facilitates neutralization and drug-sensitivity assays that use either R5 or X4 strains of human immunodeficiency virus type 1. Virology **280**:292–300.
32. **Sugden, B., K. Marsh, and J. Yates.** 1985. A vector that replicates as a plasmid and can be efficiently selected in B-lymphoblasts transformed by Epstein-Barr virus. Mol. Cell. Biol. **5**:410–413.
33. **Tisdale, M., S. D. Kemp, N. R. Parry, and B. A. Larder.** 1993. Rapid in vitro selection of human immunodeficiency virus type 1 resistant to 3′-thiacytidine inhibitors due to a mutation in the YMDD region of reverse transcriptase. Proc. Natl. Acad. Sci. USA **90**:5653–5656.
34. **Tural, C., L. Ruiz, C. Holtzer, J. Schapiro, P. Viciana, J. Gonzalez, P. Domingo, C. Boucher, C. Rey-Joly, and B. Clotet.** 2002. Clinical utility of HIV-1 genotyping and expert advice: the Havana trial. AIDS **16**:209–218.
35. **Vandamme, A. M., F. Houyez, D. Banhegyi, B. Clotet, G. De Schrijver, K. A. De Smet, W. W. Hall, R. Harrigan, N. Hellmann, K. Hertogs, C. Holtzer, B. Larder, D. Pillay, E. Race, J. C. Schmit, R. Schuurman, E. Schulse, A. Sonnerborg, and V. Miller.** 2001. Laboratory guidelines for the practical use of HIV drug resistance tests in patient follow-up. Antivir. Ther. **6**:21–39.
36. **Vodros, D., C. Tscherning-Casper, L. Navea, D. Schols, E. De Clercq, and E. M. Fenyo.** 2001. Quantitative evaluation of HIV-1 coreceptor use in the GHOST3 cell assay. Virology **291**:1–11.
37. **Willey, R. L., R. Shibata, E. O. Freed, M. W. Cho, and M. A. Martin.** 1996. Differential glycosylation, virion incorporation, and sensitivity to neutralizing antibodies of human immunodeficiency virus type 1 envelope produced from infected primary T-lymphocyte and macrophage cultures. J. Virol. **70**:6431–6436.
38. **Wilson, J. W.** 2003. Update on antiretroviral drug resistance testing: combining laboratory technology with patient care. AIDS Read. **13**:25–30, 35–38.
39. **Winters, M. A., R. J. Bosch, M. A. Albrecht, and D. A. Katzenstein.** 2003. Clinical impact of the M184V mutation on switching to didanosine or maintaining lamivudine treatment in nucleoside reverse-transcriptase inhibitor-experienced patients. J. Infect. Dis. **188**:537–540.
40. **Yoshikura, H.** 1989. Thermostability of human immunodeficiency virus (HIV-1) in a liquid matrix is far higher than that of an ecotropic murine leukemia virus. Jpn. J. Cancer Res. **80**:1–5.